Online Appendix

# Territorial control in civil wars: Theory and measurement using machine learning

June 2020

# Contents

# A Event data

The location of terrorist events and events that are indicative on conventional guerrilla fighting come from the Global Terrorism Database (GTD) and the Georeferenced Event Dataset (GED), respectively. In this section, I describe in more detail the coding decisions made in the usage of both datasets in this project.

## A.1 Minimum precision of location geocoding

The Global Administrative Areas project (`gadm.org`) provides information about country boundaries and administrative subdivisions. The division, naming, and availability varies by country, but can roughly be grouped into the following levels: level 0 (national), level 1 (state/province), level 2 (county/district), and level 3 (smaller than county or district). The GED, GTD, and ACLED event data sets reference this ordering in the administrative division of countries when specifying the of the geolocation of events. For the GED, the variable is called `where_prec` and ranges from 1 to 7 (Croicu and Sundberg, 2017). For the GTD, the variable is called `specificity` and ranges from 1 to 5 (START, 2016). Finally, the geolocation precision in the ACLED data set, that is used to construct the validation sample for the Nigeria case, is given via the variable `geo_precision` and ranges from 1 to 3 (Raleigh et al., 2010).

Table I synthesizes the precision coding of the GED, GTD, and ACLED datasets, and the inclusion into the base sample of events for analysis. As mentioned in the main text, in order to ensure a minimum level of geo-precision of the events, only events that can be attributed to at least the second order subnational administrative division are included. Specifically, this means that for GTD, precision codes 1, 2, and 3 are included, for the GED data precision codes 1, 2, and 3 as well, and for ACLED, only precision codes 1 and 2 are included in the sample. Without this limitation, events that cannot be at the minimum attributed to the county or district level would be attributed to the provincial capital or geographic center of a province — thereby biasing the event counts in smaller geographic units.

Table I. Grouping and inclusion of GTD, GED, and ACLED precision codes. The descriptions are taken from the codebooks of the GTD (START, 2016), the GED (Croicu and Sundberg, 2017), and ACLED (Raleigh et al., 2010) datasets.

| GTD | GED | ACLED | Include |
|---|---|---|---|
| 1: "city/village/town and lat/long is for that location" | 1: "Event can be related to an exact location, meaning a place name with a specific pair of latitude and longitude coordinates" | 1: "town; outskirts of a town of city" | Yes |
| | 2: "Event can be near, in the area of or up to 25 km away from an exact location, meaning a place name with a specific pair of coordinates" | | Yes |
| 2: "event occurred in city/village/town and no lat/long could be found, so coordinates are for centroid of smallest subnational administrative region identified"<br>3: "event did not occur in city/village/town, so coordinates are for centroid of smallest subnational administrative region identified" | "3: Event can be related to a second order administrative division (ADM2), such as a district, municipality or commune" | "2: small part of a region, general area; town is chosen to represent event" | Yes |
| 4: "no 2nd order or smaller region could be identified, so coordinates are for center of 1st order administrative region" | 4: "Event can be related to a first order administrative division (ADM1), such as a province, state or governorate" | 3: "Provincial capital" | No |
| | 5: "Event can only be specified to a feature that is neither a known point nor a known formal administrative division, but rather a linear feature (e.g. a long river, a border or a road) or a fuzzy polygon without defined borders (informal regions, large radiuses etc.). A representation point is chosen for the feature and employed. Similarly, if a location is only known to be between two points, and these two points are more than 25 km apart, such locations are coded with geoprecision 5." | | No |
| | 6: "Event can only be related to the whole country" | | No |
| | 7: "Event can only be related to an estimated pair of coordinates at sea or in the air (provided the airplane did not crash as a result of the event; in such cases the location of the crash is coded with the appropriate precision code)." | | No |
| 5: "no 1st order administrative region could be identified for the location of theattack, so latitude and longitude are unknown" | | | No |

## A.2 Delineating terrorism and guerrilla tactics

### A.2.1 Conceptual distinction

It is difficult to unambiguously delineate terror and non-terror tactics (Asal et al., 2012). However, the existing literature helps to outline a few general characteristics of terror versus non-terror rebel violence. Generally speaking, terrorism seeks to weaken the opponent through coercion, while guerrilla tactics are employed to weaken the enemy militarily (Bakker et al., 2016; de la Calle and Sánchez-Cuenca, 2012; Schelling, 1960). Thus, terror tactics could be characterized as approaches to weaken the enemy indirectly, while guerrilla tactics involve more direct attacks (Polo and Gleditsch, 2016; Sandler, 2014). While terrorist tactics are waged predominantly against noncombatants, guerrilla warfare targets predominantly the security forces of the state (Carter, 2016; U.S. Army/Marine Corps, 2006).[1]

The GTD database offers a comprehensive definition of terrorist attacks as "the threatened or actual use of illegal force and violence by a non-state actor to attain a political, economic, religious, or social goal through fear, coercion, or intimidation." (START, 2016: p. 10 codebook version of July 2018). In addition, at least two of the following three criteria have to be met for an event to be included in the database: a) aim at attaining a broader economic (i.e. not exclusively profit seeking), political, religious or social goal, b) convey message to larger audience than "immediate victims," and/or c) cannot be an action that would be considered a legitimate act of warfare according to international humanitarian law. (START, 2016)

[1]The Army Field Manual states: "Terrorist tactics employ violence primarily against noncombatants. Terror attacks generally require fewer personnel than guerrilla warfare or conventional warfare. They allow insurgents greater security and have relatively low support requirements. Insurgencies often rely on terrorist tactics early in their formation due to these factors. Terrorist tactics do not involve mindless destruction nor are they employed randomly. Insurgents choose targets that produce the maximum informational and political effects. Terrorist tactics can be effective for generating popular support and altering the behavior of governments. [...] Guerrilla tactics, in contrast, feature hit-and-run attacks by lightly armed groups. The primarily targets are HN government activities, security forces, and other COIN elements. Insurgents using guerrilla tactics usually avoid decisive confrontations unless they know they can win. Instead, they focus on harassing counterinsurgents. As with terrorist tactics, guerrilla tactics are neither mindless nor random. Insurgents choose targets that produce maximum informational and political effects. The goal is not to militarily defeat COIN forces but to outlast them while building popular support for the insurgency." (U.S. Army/Marine Corps, 2006: 18)

Conceptually, the most challenging aspect of distinguishing terrorist and guerrilla tactics arises with regard to the targeting of noncombatants. While all attacks against noncombatants are illegitimate within the realm of international humanitarian law, not all attacks against civilians either serve a broader socio-economic, cultural, or religious goal, and/or are intended to convey a message to an audience beyond the immediate victims of the attack. Discriminate civilian victimization, i.e. attacks against civilians that are "perceived to be directly and materially aiding the enemy" (Fortna et al., 2018: 783) should not be considered terrorism.

### A.2.2 Coding decisions

The identification of levels of territorial control in the main text relies on the distinction between events that are indicative of terrorism versus events that are indicative of the use of conventional guerrilla tactics. Terrorist events are taken from the GTD database. Events that are indicative of conventional guerrilla fighting are taken from the GED database. An insufficient mapping of the events captured in the GTD and GED databases to the conceptual distinction between terrorism and non-terror guerrilla violence, as well as an insufficient degree of separation GTD versus GED events would present a threat to identification for the model.

A number of coding choices are implemented to ensure a sufficient degree of separation:

- Limit the events from the GED database to "state-based" conflicts (`type_of_violence == 1`) and drop events classified as either "non-state conflict" or "one-sided violence." In particular the overlap between one-sided violence against civilian actors in the GED and terrorism against civilian targets in the GTD database is likely to be high. Dropping events classified as "non-state conflict" or "one-sided violence" ensures that events from the GED are indicative of direct clashes between the insurgents and the government.

- Include only events which the GTD database categorizes unambiguously as "proper terrorism" (i.e. `doubt_terr == 0`). An event that could alternatively be categorized as "1) Insurgency/Guerilla Action; 2) Other Crime Type; 3) Intra/Inter-group conflict; 4) Lack of Intentionality; or 5) State Actor" (START, 2016: p. 11 codebook version of July 2018) is excluded from the analysis.

- Exclude events from the GTD that are coded as having been targeted against the military (i.e. `targtype1_txt != "Military"`).

- As a robustness check, additionally exclude events from the GTD that are coded as "assassinations" (i.e. `attacktype1_txt != "Assassination"`), which due to the lack of the "randomness" of violence might not conform to our understanding of terrorism.

- As a robustness check, additionally exclude events from the GTD that are coded as having been targeted against "official" targets, i.e. government installations (both general and diplomatic) and police.

Thus, the subset of GED events that are included in the analysis constitute direct engagements between the rebels and state forces. The subset of GTD events that are used to identify the prevalence of terrorist tactics comprise only events that are indiscriminately directed against noncombatants or non-government institutions.

### A.2.3 Investigating overlap between GED and GTD

To investigate the degree to which the GTD and GED data overlap, use tools from the `meltt` `R` package (Donnay et al., 2019). `meltt` uses actor, precision, and event type taxonomies and user-defined spatial and temporal windows to automate the identification of potential duplicates in event data. Following (Donnay et al., 2019), I use a spatial window of 3km and a temporal window of one day to define proximate events. I focus the analysis on events in Nigeria involving Boko Haram from 2008 to 2017.[2]

[2] Boko Haram events in the GED data are identified via the `side_b` variable, specifically events mentioning "Jama'atu Ahlis Sunna Lidda'awati wal-Jihad" or "IS" as the perpetrator. Boko Haram events in the GTD data are identified via the `gname` variable, specifically events mentioning "Boko Haram" or "Al-Qaida in the

Excluding events that are coded as potentially not being terroristic (i.e. `doubt_terr == 0`) and military targets from the GTD (wide definition of terrorism), the software identifies 220 of 2838 total events, or 7.75%, as potential duplicates. Using an alternative stricter definition of terrorism from Fortna et al. (2018) that excludes official targets, maritime targets, unknown targets, and a number of attack types, 128 of a total of 2209 events, or 5.8% are identified as potential duplicates.

I hand-code the 128 potential duplicates identified by `melttt` for the stricter definition of terrorism regarding whether they are true duplicates or not. Table II displays the results. 38% of the potential matches are not duplicates upon closer investigation of the data bases and underlying source material (false positives). 43% of events are identified as duplicates (true positives). Of these 55 duplicates, 24 events (44%) should be coded as terroristic events, 13 events (24%) should be coded as non-terror violence, and 18 events (33%) could not be unambiguously identified. In 19% of the total cases it was not possible to determine whether the events matched by `melttt` constituted a true duplicate or not.

| Hand-coded category | Number of events | Percentage |
|---|---|---|
| Not a duplicate | 49 | 38% |
| Duplicate, should be terror violence | 24 | 19% |
| Duplicate, should be non-terror violence | 13 | 10% |
| Duplicate, unclear | 18 | 14% |
| Unclear | 24 | 19% |

Table II. Categorization of potential duplicates between GED and GTD data bases identified by `melttt` for Boko Haram events in Nigeria 2008–2017.

I conclude that the coding rules outlined in Section A.2.2 provide a sufficient degree of distinction between terror and non-terror insurgent violence given a) the low overall percentage of potential duplicates (5.8%), b) the even lower amount of true duplicates (2.5%, or 3.6% if unclear events are included), and c) the relative balance between terror and non-terror violence among duplicates.

Islamic Maghreb (AQIM)" as the perpetrator.

## A.3 Descriptive figures

### A.3.1 Temporal distribution of events

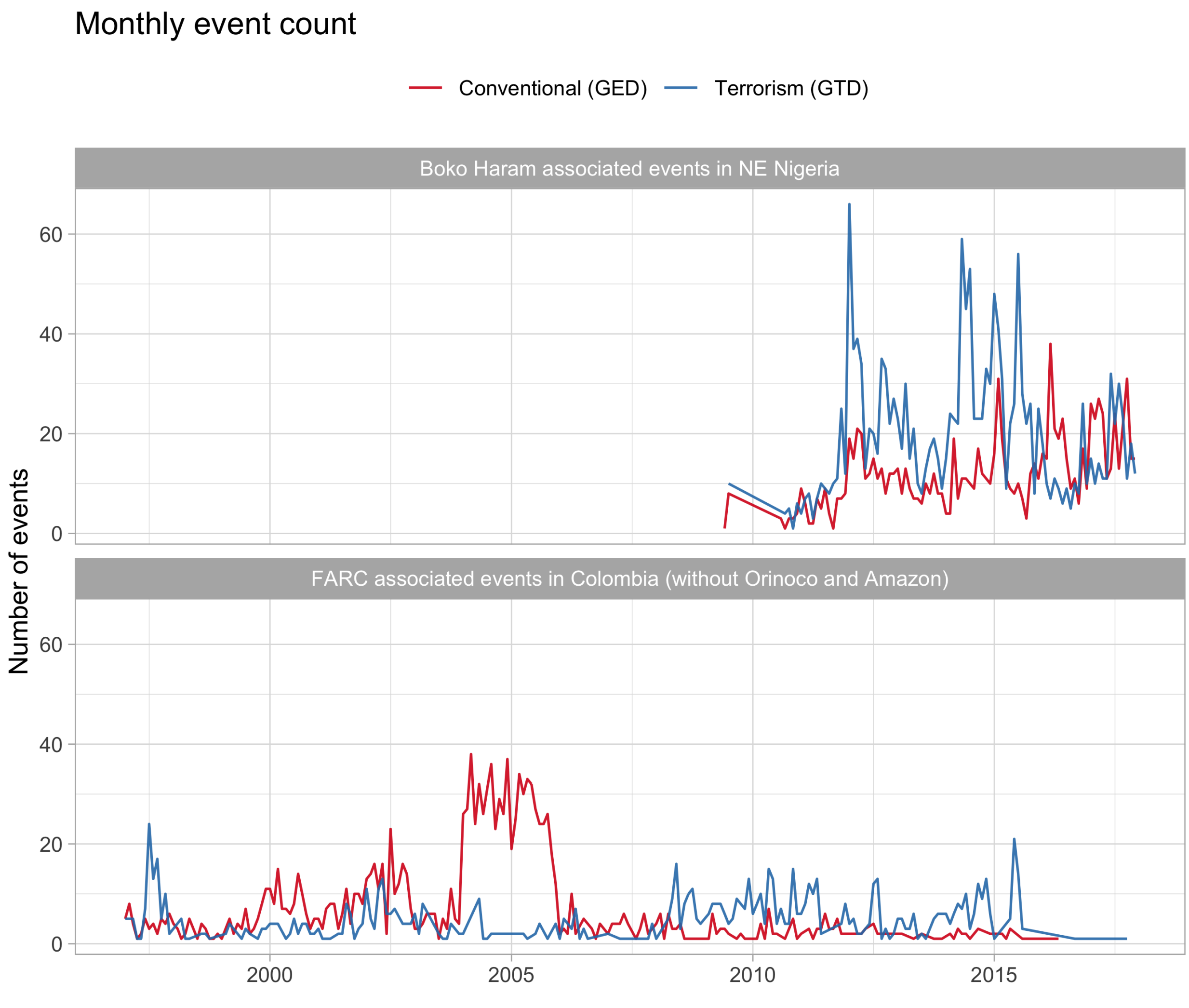


Figure 1. Monthly number of events indicating conventional guerrilla fighting (in red) versus terrorist attacks (in blue) for subregions of Colombia and Nigeria. For Nigeria, there are a total number of 1086 events that are indicative of terrorist tactics; 1123 are indicative of conventional guerrilla fighting. For Colombia, there are a total number of 1807 events that are indicative of terrorist tactics; 566 are indicative of conventional guerrilla fighting.

#### A.3.2 Spatial distribution of events

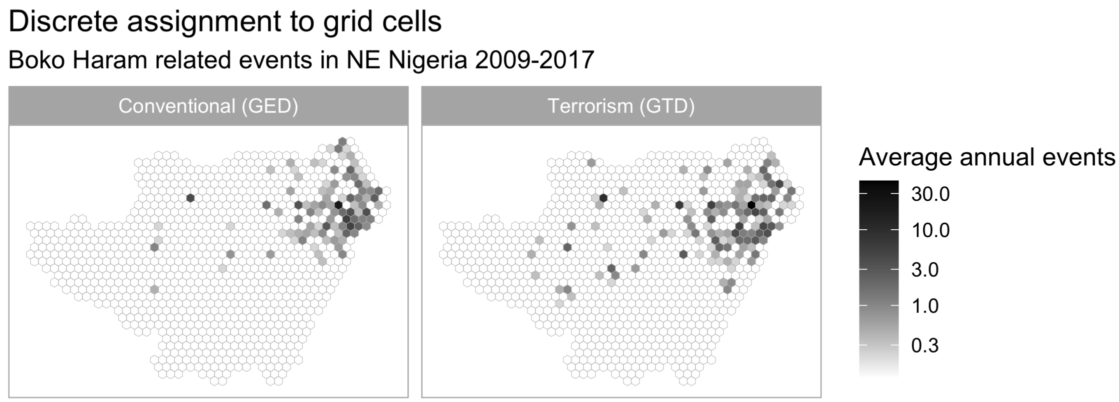


(a) Average of discrete event counts per grid cell and rebel tactic. Please note that the colors are displayed on a log scale (base 10) to make differences visually more distinguishable.

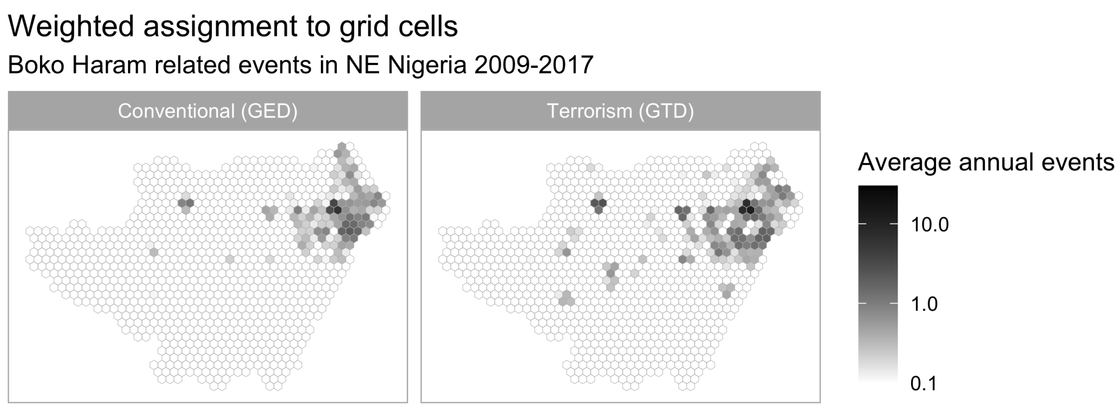


(b) Average of spatially and temporally weighted event counts per grid cell and rebel tactic. Please note that the colors are displayed on a log scale (base 10) to make differences visually more distinguishable.

Figure 2. Spatial distribution of average annual Boko Haram related events per grid cell for NE Nigerian from 2009 to 2017. There are a total of 943 grid cells in the Nigeria sample. The coverage of the data mirrors the 15 states included in the study by Aronson et al. (2017) that are most subjected to Boko Haram violence, namely Adamawa, Bauchi, Benue, Borno, Gombe, Jigawa, Kaduna, Kano, Katsina, Nassarawa, Niger, Plateau, Taraba, Yobe, and the Federal Capital Territory. The upper panel plots the average of discrete event counts; the lower panel plots the average weighted events. While the numerical values are lower, the general patterns of the spatial distribution of events remain intact upon spatially and temporally weighting events to compute a grid cell's conflict exposure. See Online Appendix Section B for more details on the weighting procedure.

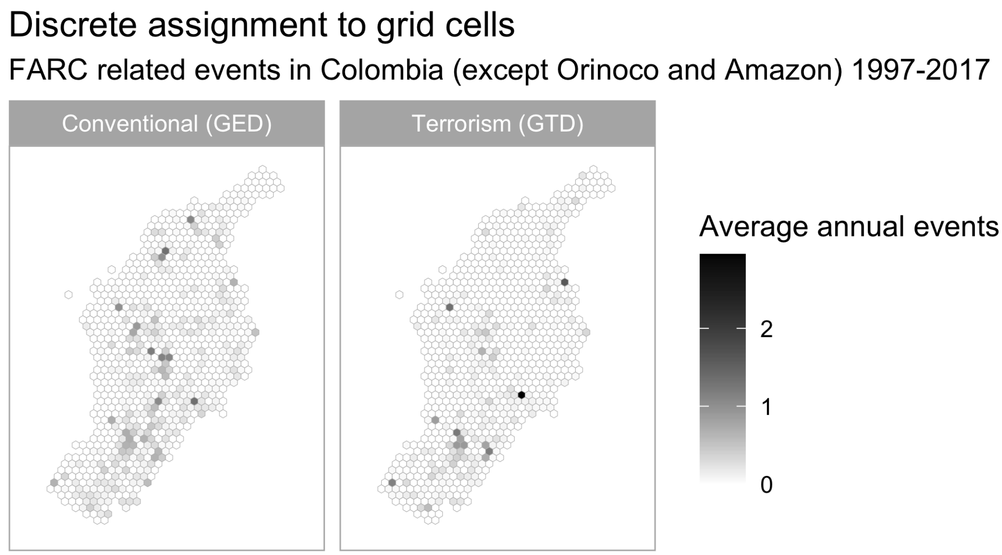


(a) Average of discrete event counts per grid cell and rebel tactic.

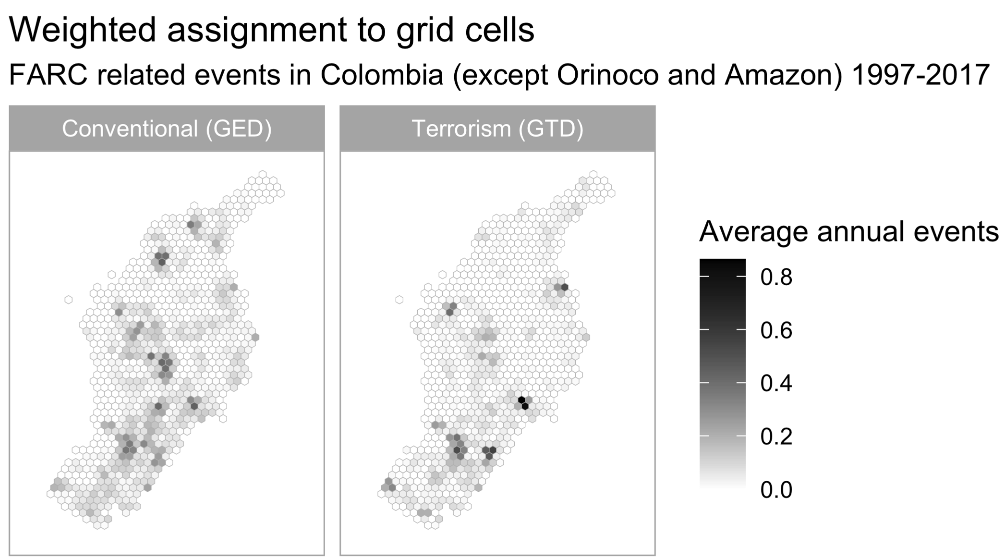


(b) Average of spatially and temporally weighted event counts per grid cell and rebel tactic.

Figure 3. Spatial distribution of average annual FARC related events per grid cell for Colombia from 1997 to 2017. There are a total of 851 grid cells in the Western Colombia sample. The upper panel plots the average of discrete event counts; the lower panel plots the average weighted events. While the numerical values are lower, the general patterns of the spatial distribution of events remain in tact upon spatially and temporally weighting events to compute a grid cell's conflict exposure. See Online Appendix Section B for more details on the weighting procedure.

# B Measuring conflict exposure

Spatially and temporally disaggregated conflict event data is a key source of information in the study of subnational violence. However, many covariates of interest operate on an areal level, for example economic wealth, terrain, the ethnic composition of the population, the availability of natural resources, or the provision of public services. Individual conflict events are thus typically aggregated to grid cells or administrative units such as districts or municipalities to match the unit of measurement of the covariates and to measure the exposure of these subnational areas to conflict events. Each conflict event is commonly assigned *discretely* to the subnational area within which it is located. This standard practice is problematic for two main reasons. First, scholars are frequently only accounting for events that fall within the boundaries of a chosen subnational unit and do not account for events that happen in the vicinity. Second, inferences regarding an area's exposure to conflict are highly sensitive to the drawing of boundaries — widely cited in the literature as the modifiable areal unit problem (MAUP, see Openshaw and Taylor 1979). A similar issue arises in the temporal domain when conflict events are discretely assigned to the calendar month or year in which they occurred. An event's influence on local conflict dynamics is unlikely to abruptly stop at the chosen spatial or temporal boundaries; nor will it homogeneously affect the entirety of the space. Rather, its impact dissipates *continuously* over space and time.

A simplistic approach to coding areas' exposure to terrorism conflict events would sum the number of events that fall within a given grid cell. This procedure faces the problem that the assignment of conflict events to grid cells is highly dependent on the sampling of centroid locations. MAUP describes the discrepancy between real world spatial patterns of events and patterns created via aggregation of events into homogenous spatial units (Openshaw and Taylor, 1979). Shifting the location of the centroids can have a severe influence on the number of events that are assigned to a particular cell. This is particularly concerning when the drawing of grid cell boundaries leads clusters of events to be broken up into smaller groups — causing the relative frequency of terrorist events and conventional war acts to change dramatically. Figure 4 illustrates this issue. Based on the location of grid cell centroids in panel A, we would code the relative frequency of rebel and conventional war fighting to correspond to the values of the variable Tactics$_{it}$ $= [D, D, A]$. If the centroids were shifted by 25% relative to the location of the events, we would conclude the emissions of these three cells to have values of Tactics$_{it}$ $= [B, D, C]$.

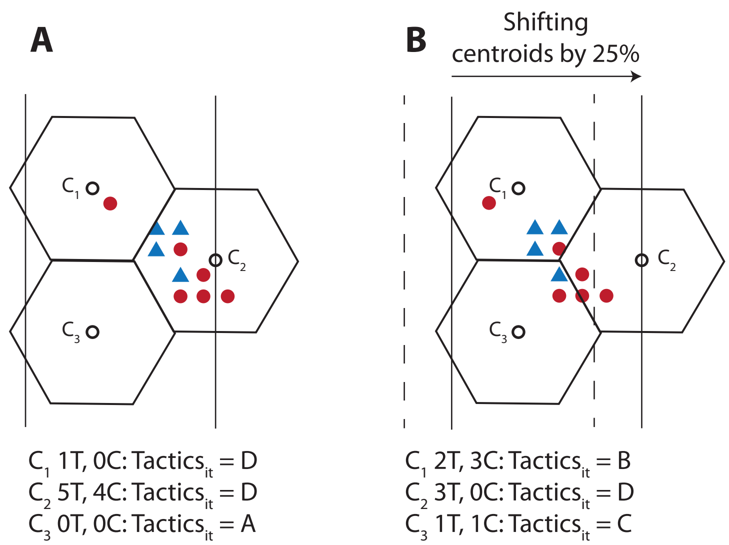


Figure 4. The schematic illustrates how shifting the location of the grid cell centroids from their original (randomly sampled) location (panel **A**) by just 25% (panel **B**) can result in vastly different conclusions about the coding of rebel tactics. Red dots indicate the location of conventional events; blue triangles those of terrorist attacks. This is a simplified example—in the analysis, Tactics$_{it}$ is computed using probabilities from Poisson distributions under application of a margin parameter.

To alleviate this problem, I propose a novel measurement model for rebel tactics in civil war that uses spatial and temporal weights to associate conflict events with grid cells rather than relying on discrete assignment. The importance of individual violent events for the estimation of territorial control decreases over time and space. I model this intuition by assigning space- and time-varying weights to each event.

For each grid cell centroid-month $c_{it}$, $i = 1, \ldots I$ indexes centroids and $t = 1, \ldots T$ indexes months. For each conflict event $e_{jm}$ , $j = 1, \ldots J$ indexes individual events and $m = 0, \ldots M$ indexes the calendar month in which the event occurred. Let $lon_i$ and $lat_i$ denote the longitude and latitude of each grid cell centroid $c_i$ in radians, respectively. Similarly, let

$lon_j$ and $lat_j$ denote the longitude and latitude of each conflict event $e_j$ in radians. Then the spatial distance $d_{ij}$ in km between centroid $c_i$ and event $e_j$ is computed as the geodesic distance between two points using the Haversine formula,

$$d_{ij} = 2r \arcsin\left(\sqrt{\sin^2\left(\frac{lat_j - lat_i}{2}\right) + \cos(lat_i)\cos(lat_j)\sin^2\left(\frac{lon_j - lon_i}{2}\right)}\right),$$

where $r \approx 6371$ denotes the earth mean radius in km. The temporal distance (in the following called age) $a_{tm} = t - m$ measures the months between when event $e_{jm}$ occurred and the time of observation of the grid cell-month $c_i t$. An event occurring in the month of observation has an age of $a_{tm} = 0$, while an event that occurred four months ago has an age of $a_{tm} = 3$.

For each centroid-month unit $c_{it}$ I measure the spatial distance $d_{ij}$ in km and the temporal distance $a_{tm}$ to each conflict event $e_{jm}$, resulting in a total number of centroid-event-month observations of size $K = I \times J \times T$. Specifically, for each grid cell $c_i$ in each month $t$, I create a vector $D$ of spatial distances and a vector $A$ of temporal distances to each event. Events that occur in the future from the time of observation t (i.e. where $u > t$) receive a missing value. I then weight both vectors to allow the impact of conflict events on grid cells to dissipate over space and time.

I assume the impact of an event to dissipate following a logistic decay function of the general form

$$w = \frac{1}{1 + e^{-\kappa + \gamma x}},$$

where $x$ denotes the decaying quantity (here event age or distance between the event and a centroid), $\kappa$ determines the slope of the curve and $\gamma$ defines its inflection point. To describe a decay function, both the slope parameter $\kappa$ and he inflection parameter $\gamma$ have to be positive real numbers. To model spatial decay, assume the slope parameter to be $\kappa_d = 7$ and the inflection parameter to be $\gamma_d = 0.35$. To model temporal decay in months, I use a steeper sigmoid curve. I assume the temporal slope parameter to be $\kappa_a = 8$ and the inflection parameter to be $\gamma_a = 2.5$.

Figure 5 plots the decay functions using these parameter values. Based on the shape of the logistic decay functions above, an event that occurs at the location of the centroid of a grid cell receives a spatial weight of 1. An event that occurs 10km away from the centroid receives a weight of 0.97 and an event 25km away is weighted by 0.15—after which its influence tends toward 0. The temporal weight features a different rate of decay. In the first month, the event receives a temporal weight of 1, followed by 0.95 in the second, 0.62 in the third, and 0.11 in the fourth month; after which the weight approaches zero.

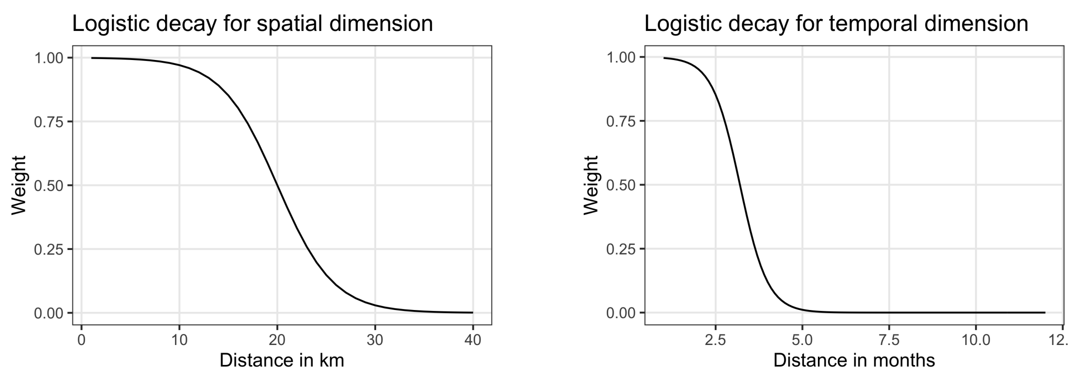


(a) Spatial

(b) Temporal

Figure 5. Logistic function that describes the decay of the influence of an event in relation to a centroid in the spatial and temporal dimensions.

The exposure of grid cell $c_{it}$ to conflict events $E_{it}$ is computed as the sum over all temporally and spatially weighted events $J$.

$$E_{it} = \sum_{j=1}^{J} \left( w_{d_{ij}} \times w_{a_{jt}} \right) \tag{1}$$

Thus, the resulting unit of observation is the grid cell-month, i.e. a vector of exposure values of size $E = I \times T$.

# C Estimation procedure

For each grid cell $i$, the following procedure is used to estimate the most probable sequence of territorial control over all time periods $t$.

1. Compute the exposure of the grid cell $i$ in month $t$ to terrorist events $E_{it}^{T}$ and to conventional war acts $E_{it}^{C}$ to all events $J$, by
   (a) computing the spatial distance $d_{ij}$ of each event $j$ to the centroid of grid cell $i$ in kilometers and weighting it using a logistic decay function,
   (b) computing the temporal distance (each event's age) $a^{jt}$ between the month $m$ when the event occurred and the time of observation of the grid cell $t$ in months and weighting it using a logistic decay function (note that only positive temporal distances $a^{jt}$ are considered), and
   (c) summing the product of the spatial and temporally weighted distances for terrorist and conventional events for each grid cell-month to arrive at $E_{it}^{T}$ and $E_{it}^{C}$. Note that spatially- and temporally weighted sums of under 0.05 in a grid cell-month are set to zero to avoid later grid-cell months having inflated cumulative event exposures.
2. For each grid cell $i$ in each month $t$, determine the value of the variable $\mathrm{o}_{it} = f\left(E_{it}^{T}, E_{it}^{C}\right)$.
3. For each grid cell $i$ in each month $t$, create a sequence of observed outputs $\mathbf{O} \in \{O1, O2, O3, O4\}$, where an individual observation $o_{it}$ is determined by $\text{Tactics}_{it}$.
4. For each grid cell $i$ compute the most probable sequence of latent states $\mathbf{Q} \in \{R, DR, D, DG, G\}$ over all time periods $t$, given the sequence of observed indicator of rebel tactics $\mathbf{O}$ over all time periods $t$, the time-invariant matrix of transition probabilities $\Theta$, and the time-invariant matrix of emission probabilities $\Phi$ via a Hidden Markov Model.

# D Model parameters

## D.1 Transition probabilities

The matrix of transition probabilities (main text Table III) is obtained from observed transitions between zones of territorial control during the Greek civil war (Kalyvas, 2006: 277). Using interviews, judicial archives, and secondary sources from two counties in the Argolid region during the Greek civil war, Kalyvas (2006) constructs a dataset of territorial control at the village level. Broadly, the following patterns are observed in the empirical data from the Greek civil war:

- Transitions from complete rebel to complete government control (and vice versa) are "almost nonexistent" (Kalyvas, 2006: 277).
- Consolidation of control from an area that is contested but closer to either the government or the rebels are "less prevalent than expected" (Kalyvas, 2006: 277).
- Situations of contested control are highly unstable and tend to shift to a situation of contested control with the government having the upper hand in the next period (Kalyvas, 2006: 277).
- Government forces are able to consolidate their control at a higher rate than insurgents (Kalyvas, 2006: 277).

Figure 6 below compares the distribution of transition probabilities from Kalyvas' empirical observations (on the left)[3] with the modified version used in the estimation of territorial control in the main manuscript (on the right). In the original matrix of transition probabilities, a number of theoretically possible transitions, for example from full rebel to full government control, are never observed. This would indicate a transition probability $P(G|R) = 0$. However, while areas are unlikely to transition from one extreme on the spectrum of territorial control to another without at least temporarily experiencing contestation,

[3] See Table 9.7 in Kalyvas (2006: 277).

it is not impossible. Therefore, the transition probabilities presented in Table III are modified from Kalyvas's empirical results to allow for all possible transitions between states to have non-zero probabilities. I make small adjustments in the numerical values to allow for a minimum transition probability of 2.5% between all possible states of territorial control.[4] The overall patterns of possible transitions remain unchanged, as illustrated in Figure 6.[5]

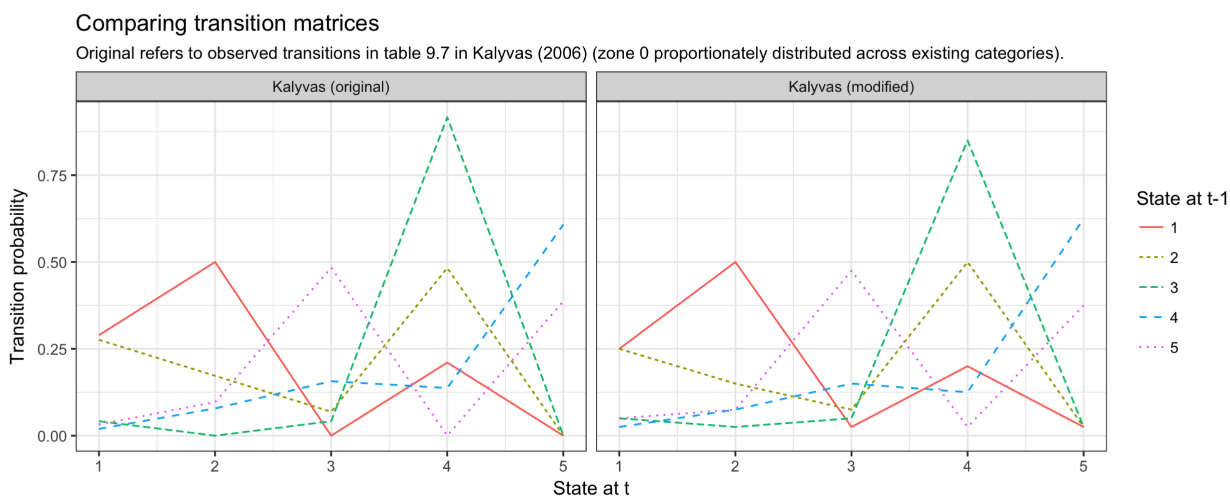


Figure 6. The figure compares the distribution of transition probabilities between the empirical observations from Kalyvas (2006) and the modified transition probabilities in this paper. The graph shows that while the transition probabilities differ slightly, the patterns of transitions between states from $t-1$ to $t$ remain unchanged.

[4]Please note the differences in presentation. Kalyvas (2006) labels zone 1 as complete government control and zone 5 as complete rebel control, while the scale in the main paper starts with rebel control $R$. Similarly, the transition matrix in Kalyvas (2006: 277) is displayed with "To" (i.e. $q_t$) in the rows and the "From" (i.e. $q_{t-1}$) in the columns. I reverse this order in the main text.

[5]Kalyvas's empirical transition matrix contains a row with transitions to a territorial control zone of value "0." No further explanation is given what this zone entails. Therefore, I spread the relative frequency of observations of a transition to zone 0 proportionately across zones 1 through 5.

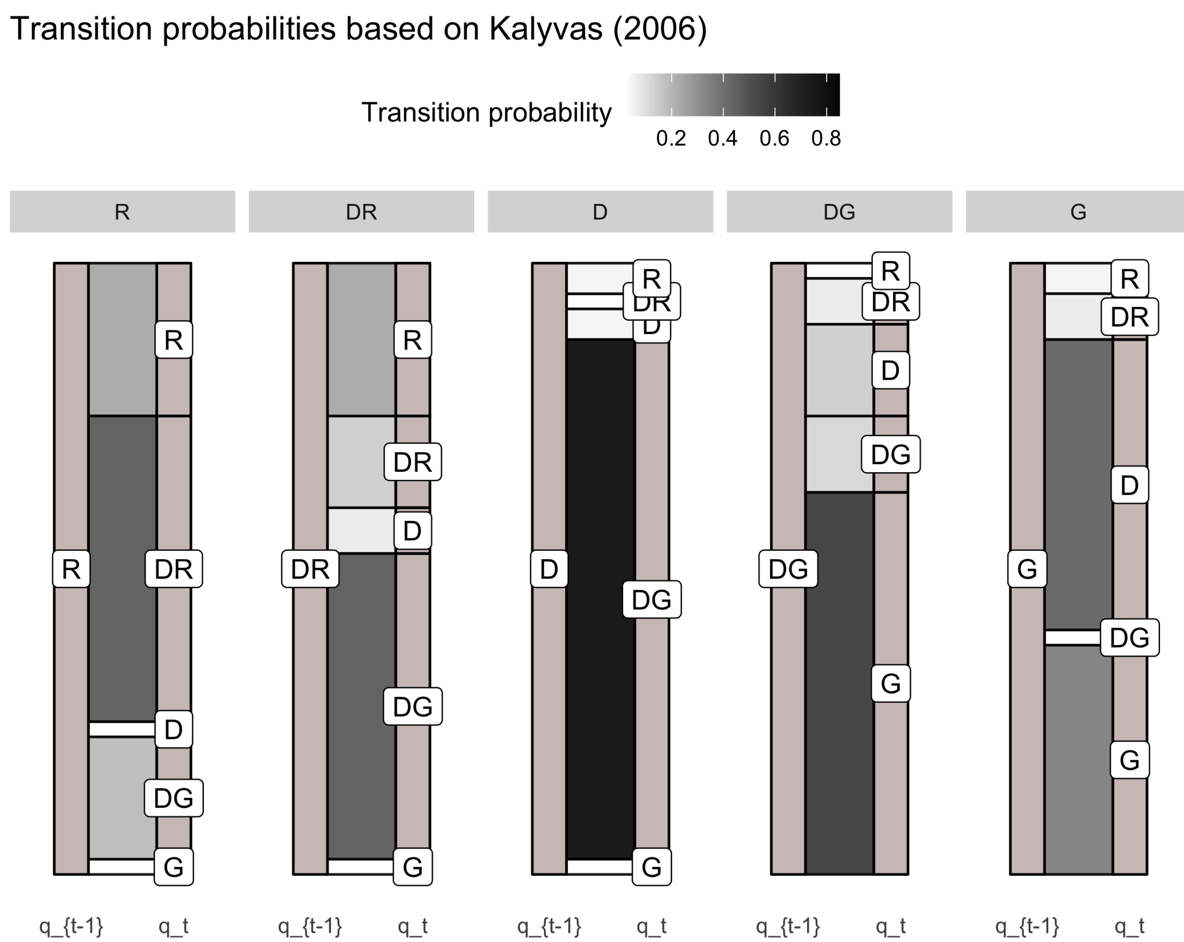


Figure 7. Illustration of modified transition probabilities from Kalyvas (2006). Colors and the height of the vertical bars indicate probabilities. Each panel illustrates the transition probabilities for a specific value of $q_{t-1}$, i.e. the most likely state of territorial control in the previous time step. For example, if an area was highly disputed ($D$) at $q_{t-1}$ (i.e. the middle panel), the area will transition to be under full rebel control ($R$) at time $q_t$ with a probability of 0.05, become disputed but closer to rebel control ($DR$) with probability 0.025, remain highly disputed ($D$) with probability 0.05, transition to disputed but closer to government control ($DG$) with probability 0.85, and be fully controlled by the government ($G$) with probability 0.025.

## D.2 Emission probabilities

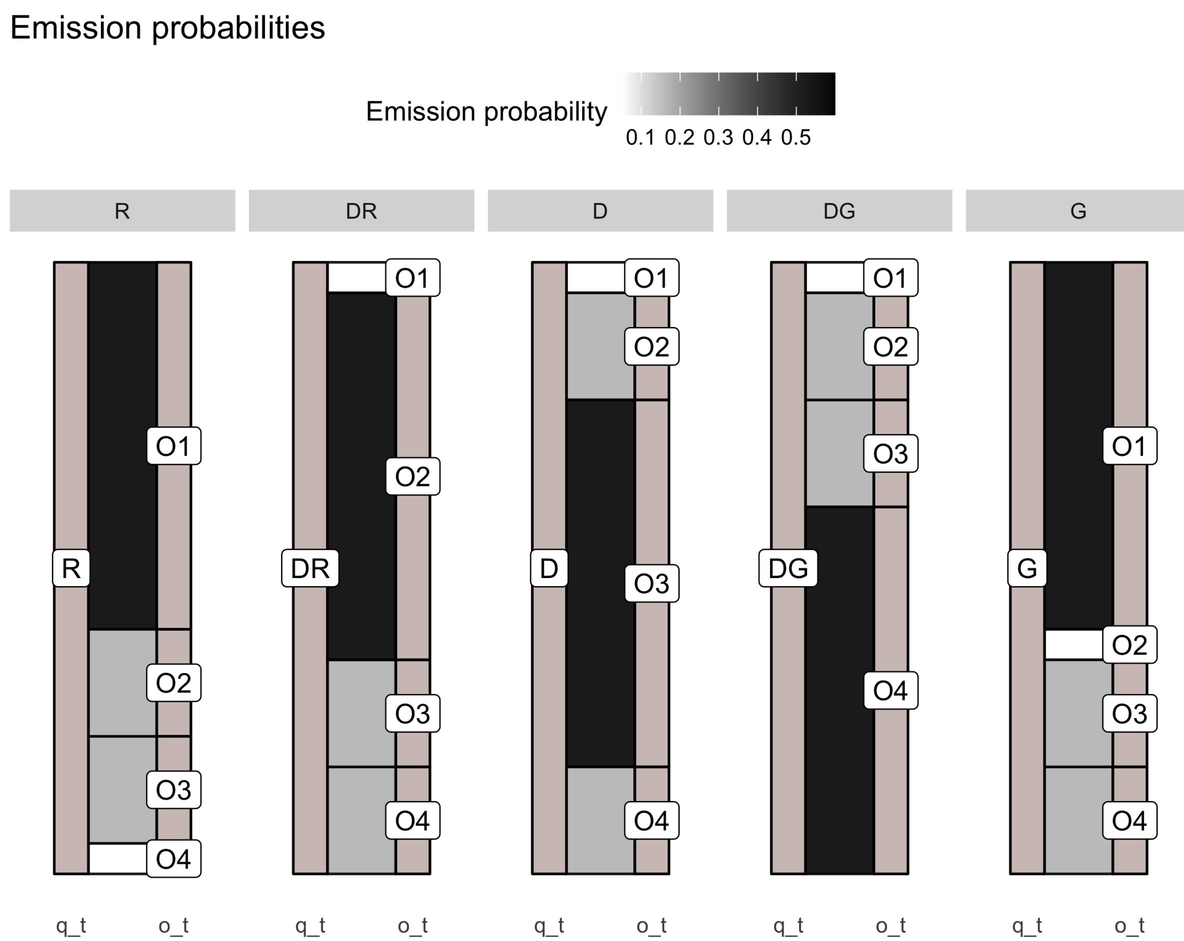


Figure 8. Illustration of emission probabilities. Colors and the height of the vertical bars indicate probabilities. Each panel illustrates the emission probabilities (i.e. the probability of observing a specific combination of rebel tactics) for a specific contemporaneous value of the unobserved state of the variable territorial control $q_t$. For example, if the true but unobserved state of an area was highly disputed ($D$) at $q_t$ (i.e. the middle panel), I expect to observe no violence ($O1$) with probability $o_t = 0.05$, more guerrilla tactics relative to terrorism ($O2$) with probability $o_t = 0.175$, a similar magnitude of tactics fighting and terrorism ($O3$) with probability $o_t = 0.6$, and more terrorism than guerrilla tactics ($O4$) with probability $o_t = 0.175$.

# E Validation via deforestation rates in Colombia

## E.1 Data sources

Raster data on deforestation from 2013 to 2016 are obtained via the forest monitoring system from the Colombian *Instituto de Hidrología, Meteorología y Estudios Ambientales* (IDEAM). IDEAM provides data on the change of forest cover obtained via Landsat 7 and 8 satellite images. The data are obtained as individual geoTIFF raster images via the IDEAM Geoserver.[6] Deforestation is defined if a pixel changes from "forest" to "no forest" within a year of observation (Cabrera et al., 2011: 26). To obtain a binary indicator of deforestation for the resolution of the 0.25 decimal degree minimum diameter hexagonal grid cells for the validation exercise in the main text, I code whether any of the pixels contained within a hexagonal grid cell experience deforestation from one year to the next, or not.

## E.2 Summary statistics for deforestation model

| Statistic | N | Mean | St. Dev. | Min | Pctl(25) | Pctl(75) | Max |
|---|---|---|---|---|---|---|---|
| $\text{Control}_{i,t}$ | 3,404 | 0.9783 | 0.0755 | 0 | 1 | 1 | 1 |
| $\Delta\text{Control}_{i,t}$ | 3,404 | 0.0062 | 0.0895 | −1 | 0 | 0 | 1 |
| $\text{Peace}_{t}$ | 3,404 | 0.2500 | 0.4331 | 0 | 0 | 0.2 | 1 |
| $\text{Deforestation}_{i,t}$ | 3,404 | 0.0496 | 0.2172 | 0 | 0 | 0 | 1 |

Table III. Summary statistics for the logistic regression model of deforestation in Colombia on changes in territorial control as a result of the 2016 peace agreement. The unit of analysis for territorial control is annual averages of monthly-level estimates for 0.25 degree hexagonal grid cells.

[6] See `http://geoapps.ideam.gov.co:8080/geoserver/web/`.

## E.3 Robustness checks

Table IV presents the main deforestation model (columns 1 to 3) and two robustness checks based on subsamples of the original data.[7] In columns 4 to 6, assassinations are excluded from the computation of subnational conflict exposure to terrorism (GTD data) before estimating territorial control via HMM. The model is robust to this exclusion and the estimates effect size of peace-induced changes of territorial control on the probability of deforestations remains approximately the same. In columns 7 to 9, I additionally exclude all government targets (i.e. general and diplomatic government targets and police) from the computation of a cells exposure to terrorism before estimating territorial control. This change causes the estimated effect size to almost double compared to the baseline model (column 8). However, the effect seizes to be statistically significant at the minimum 5% level of significance upon inclusion of a lagged dependent variable (column 9).

| | Deforestation$_{i,t}$ | | | | | | | | |
|---|---|---|---|---|---|---|---|---|---|
| | Base sample | | | Exclude assassination | | | Exclude government targets | | |
| | (1) | (2) | (3) | (4) | (5) | (6) | (7) | (8) | (9) |
| $\Delta$Control$_{i,t}$ × Peace$_t$ | | 3.59$^{*}$ | 3.29$^{*}$ | | 5.07$^{*}$ | 4.73$^{*}$ | | 6.20$^{*}$ | 4.22 |
| | | (1.68) | (1.63) | | (2.28) | (2.19) | | (2.53) | (2.57) |
| $\Delta$Control$_{i,t}$ | −0.63 | −1.51 | −1.56 | −0.58 | −2.26 | −2.24 | −2.36 | −3.80$^{*}$ | −2.33 |
| | (1.00) | (0.97) | (0.86) | (1.52) | (1.58) | (1.51) | (1.80) | (1.63) | (1.77) |
| Peace$_t$ | 0.29 | 0.22 | 0.07 | 0.29 | 0.21 | 0.05 | 0.32$^{*}$ | 0.25 | 0.08 |
| | (0.16) | (0.16) | (0.18) | (0.16) | (0.17) | (0.18) | (0.16) | (0.17) | (0.18) |
| Deforestation$_{i,t-1}$ | | | 0.86$^{**}$ | | | 0.85$^{**}$ | | | 0.86$^{**}$ |
| | | | (0.28) | | | (0.28) | | | (0.28) |
| Constant | −3.03$^{***}$ | −3.04$^{***}$ | −2.94$^{***}$ | −3.03$^{***}$ | −3.04$^{***}$ | −2.94$^{***}$ | −3.04$^{***}$ | −3.05$^{***}$ | −2.94$^{***}$ |
| | (0.10) | (0.10) | (0.11) | (0.10) | (0.10) | (0.11) | (0.10) | (0.10) | (0.11) |
| Observations | 3,404 | 3,404 | 2,553 | 3,404 | 3,404 | 2,553 | 3,404 | 3,404 | 2,553 |
| Log Likelihood | −670.74 | −668.87 | −545.38 | −670.88 | −668.61 | −545.30 | −669.56 | −667.34 | −545.99 |
| Akaike Inf. Crit. | 1,347.48 | 1,345.73 | 1,100.75 | 1,347.75 | 1,345.22 | 1,100.59 | 1,345.13 | 1,342.67 | 1,101.98 |

*Note:* $^{*}$p<0.05; $^{**}$p<0.01; $^{***}$p<0.001

Logistic regression coefficients with bootstrapped clustered standard errors by grid cell in parentheses.

Table IV. Relationship between rebel territorial control and deforestation in Colombia.

[7] See online appendix Section A.2.2 for more detail.

# F Validation via ACLED data in Northeast Nigeria

The coverage of the HMM results mirrors the 15 states included in the study by Aronson et al. (2017) that are most subjected to Boko Haram violence, namely Adamawa, Bauchi, Benue, Borno, Gombe, Jigawa, Kaduna, Kano, Katsina, Nassarawa, Niger, Plateau, Taraba, Yobe, and the Federal Capital Territory.

Through event type labels, ACLED contains information on whether an event resulted in rebels gaining control or establishing a base (coded as R, continuous value 0), battles with no changes in control (D, continuous value 0.5), the government gaining control or establishing a base (G, continuous value 1), and instances of remote violence (DR for government remote violence with a continuous value 0.25; DG for insurgent remote violence mapped to continuous value of 0.75).[8]

The events are aggregated to grid cells on a monthly level. Territorial control is assigned based on the occurrence of control-related events within a grid cell. New events cause a cell to update the coded level of territorial control based on event type. In the case of multiple events occurring in the same grid cell month, I average across them. In the main specification, cells with no events in a given month are imputed to mirror the previous month's control up to a duration of six months, unless a new event is observed. If a cell does not experience any violence in the previous six months, it is assumed to be under government control. Cells that experience zero events over the entire period of observation 2008 to 2017 are assumed to be under full government control.

In the robustness checks below, I also construct ACLED validation sets in which the window of lags for imputation and/or the switching to a label of full government control is reduced to three months, or increased to twelve months, respectively.

I create validation data with two alternative translations of ACLED event labels to levels

[8]Similar coding procedures have been used by Sauter (2017) and Wimmer and Miner (2019). ACLED contains a small number of events for which manual coding is necessary to determine the actor gaining control, in particular for occurrences of remote violence. The respective documentation is available upon request.

of territorial control. The first validation set adopts the assumption that remote violence is indicative of areas that are disputed, but closer to either rebel or government control, depending on the perpetrator (denoted “full sample” below). The second data set drops this assumption and considers only ACLED events that make explicit reference to changes in territorial control (denoted “restricted sample” below). Table V outlines the events that are included in the construction of each validation set. Figure 9 below plots yearly averages for both validation data sets for the 6-month threshold, Figure 10 plots the same for the 12-month threshold. The graphs illustrate the the average level of rebel control is higher if a higher temporal threshold for lags and the reversion to government control is used in the construction of the validation set.

| **ACLED category** | **Coding** | **Notes** | **Full sample** | **Restricted sample** |
|---|---|---|---|---|
| Battles - No change of territory | Contestation | | x | x |
| Battle - Government regains territory | Government control | | x | x |
| Battle - Non-state actor overtakes territory | Rebel control | | x | x |
| Headquarters or base established | Government or rebel control (depending on actor) | | x | x |
| Non-violent transfer of territory | Government or rebel control (depending on actor) | | x | x |
| Remote violence | Contested, closer to government | Similar to terrorism | x | |
| Strategic development | Contested, closer to government or rebels (depending on actor) | Indicates at least presence of actor | x | |
| Violence against civilians | | | | |
| Riots/Protests | | | | |

Table V. Overview over inclusion and categorization of ACLED events in the construction of the validation data. Events coded as riots/protests, as well as violence against civilians are excluded. Remote violence and instances of strategic development are dropped in the restricted validation set.

## F.1 Robustness checks

Figure 11 plots monthly-level Spearman’s correlation coefficients for the HMM estimates for NE Nigeria and six alternative codings of the ACLED validation data, with loess smoothed

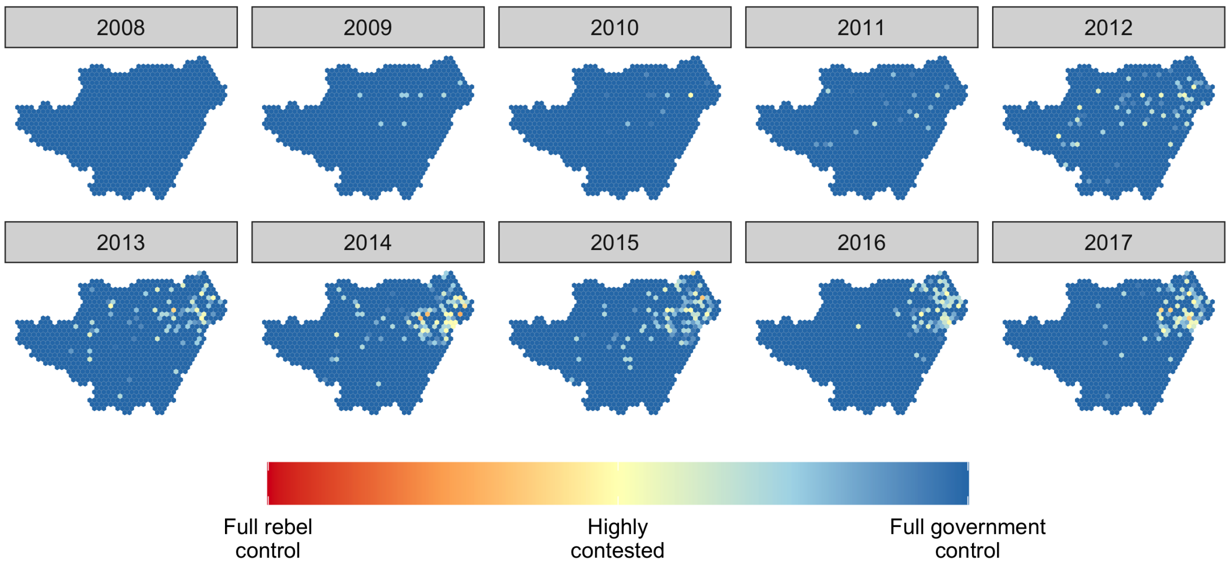


(a) Full set of ACLED event types

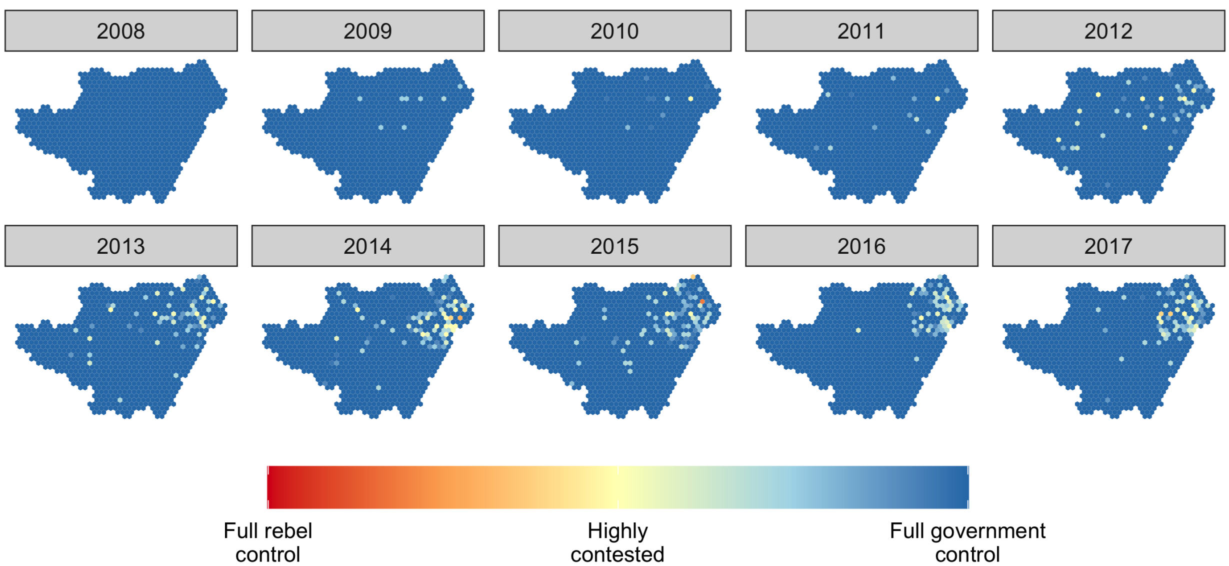


(b) Subset of ACLED event types (more restrictive)

Figure 9. Yearly averages of monthly-level ACLED validation data values. Values that are closer to 0 indicate full rebel control; values closer to 1 full government control. 0.5 indicates cells that are highly disputed. If a cell does not experience any violence in the previous 6 months, it is assumed to be under government control.

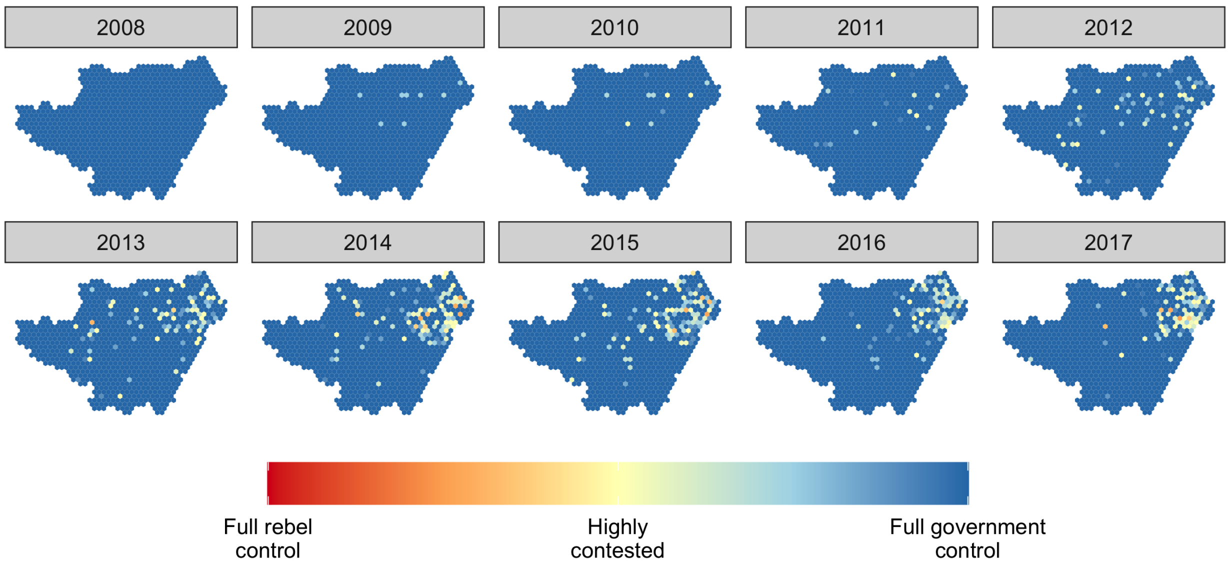


(a) Full set of ACLED event types

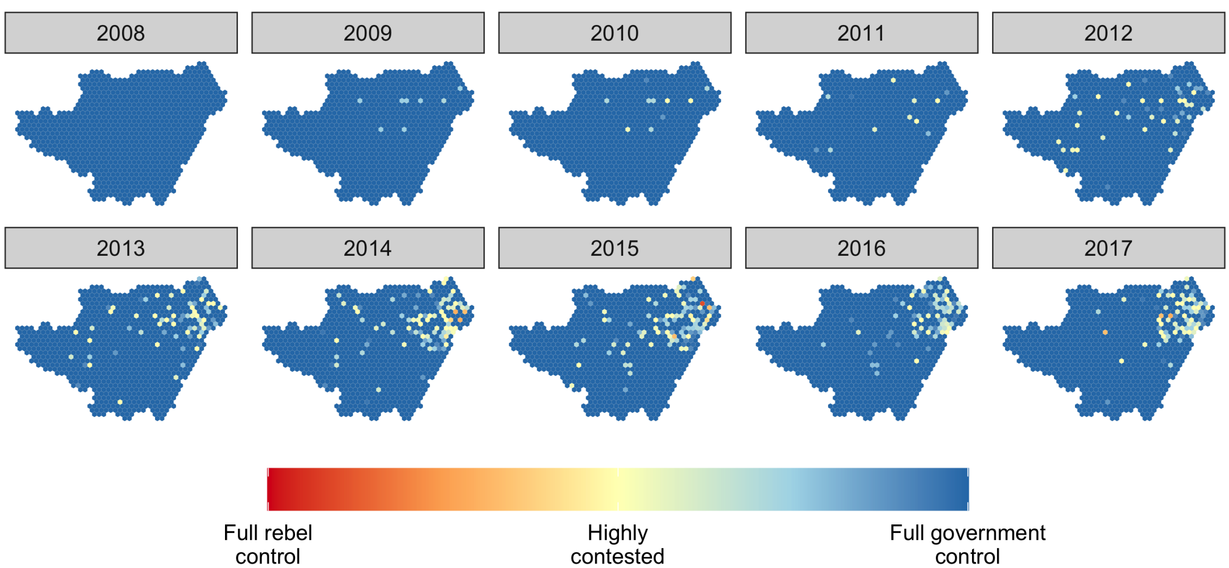


(b) Subset of ACLED event types (more restrictive)

Figure 10. Yearly averages of monthly-level ACLED validation data values. Values that are closer to 0 indicate full rebel control; values closer to 1 full government control. 0.5 indicates cells that are highly disputed. If a cell does not experience any violence in the previous 12 months, it is assumed to be under government control.

trend lines. The "full" sample is shown in black. The more conservative coding of the "restricted" sample is shown in grey. The graph shows that the "full" sample on average yields slightly higher correlations with the HMM estimates than the more restricted sample. However the difference is small and does not appear to be statistically significant based on the loess smoothed trend lines.

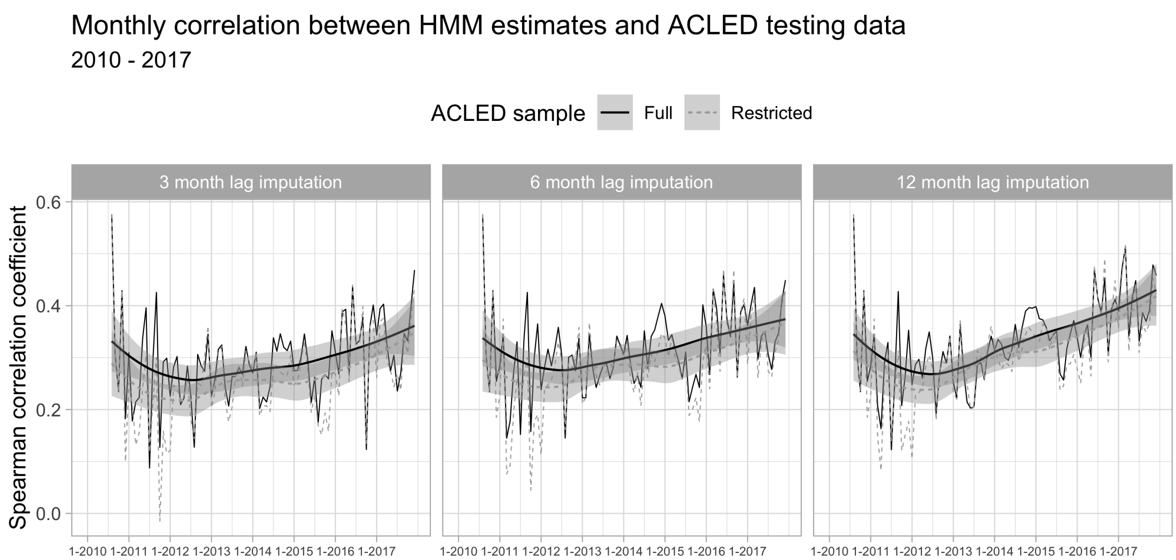


Figure 11. Spearman's correlation coefficients for monthly correlations between HMM estimates and the ACLED validation data, including loess smoothed average.

The left-most panel in Figure 11 plots the correlations with ACLED data for which a 3-month upper bound is adopted to cause a grid cell with no conflict events to be coded as being under government control. The middle panel plots the results for a the same analysis using a six-month upper bound, and the right-most panel shows the correlations for the 12-month window. Across all three version of the data, a larger time window is associated with a higher correlation between the HMM estimates and the ACLED data, however, the differences are very small. A larger time window means that grid cells in the ACLED validation set which are not coded as 1 (i.e. full government control) stay below 1 for a longer period of time, thus increasing the average level of Boko Haram control and decreasing the average level of government control.

## F.2 Distribution

Figure 12 and Table VI show the distribution of territorial control values for the HMM estimates and the ACLED validation data. The original ACLED validation set contains a larger number of possible bins because multiple observations occurring in the same grid-cell month are averaged. To make the distribution more comparable, I re-bin the ACLED validation set.

$$\text{ACLED re-binned} = \begin{cases} 0, & \text{, if ACLED } < .125 \\ .25, & \text{, if ACLED } \leq .125 \text{ \& ACLED } < .375 \\ .5, & \text{, if ACLED } \leq .375 \text{ \& ACLED } < .625 \\ .75, & \text{, if ACLED } \leq .625 \text{ \& ACLED } < .875 \\ 1, & \text{, if ACLED } \leq .875 \end{cases}$$

As mentioned in the main manuscript, due to the strong assumptions necessary for constructing validation data from ACLED, as well as concerns regarding reporting error in these data (Eck, 2012), the comparison with the HMM estimates should be taken with a grain of salt. In particular, not every event in the ACLED data base can unambiguously be linked to a specific status or change in the territorial control on the ground. Thus, the validation data constructed from ACLED likely understates the extent of rebel control and overstates the extent of government control. However, the testing set constructed from ACLED data offers the best opportunity for out-of-sample validation of territorial control in Nigeria available to date.

Comparing the HMM estimates and the re-binned version of the ACLED validation data shows that the HMM estimates yield higher levels of complete rebel control and areas that are disputed but closer to rebel control, as well as areas that are disputed but closer to government control, as compared with the ACLED validation set. The HMM appears to underestimate the level of full government control in NE Nigeria over the period of observation.

| Territorial control | HMM | ACLED re-binned (6m) | ACLED re-binned (12m) |
|---|---|---|---|
| 0.00 | 0.64 | 0.09 | 0.11 |
| 0.25 | 1.11 | 0.11 | 0.14 |
| 0.50 | 2.38 | 1.95 | 2.79 |
| 0.75 | 2.87 | 0.54 | 0.77 |
| 1.00 | 93.00 | 97.31 | 96.19 |

Table VI. Comparison of the percentage of grid-cell months associated with a specific value of territorial control for the HMM estimates and re-binned versions of ACLED (using the 'full' specification).

## F.3 Comparison with Reuters maps

Detailed information about *changes* of territorial control over time is extremely hard to find. To the best knowledge of the author, the maps by Reuters re-produced in Figure 1 in the main text offer the best opportunity for further validation of changes in territorial control. These maps no not represent a "ground truth" of territorial control, because their level of aggregation is rather high. However, they offer the most consistent information about changes in territorial available.

As mentioned in footnote 8 on page 6 of the main text, the map in Figure 1 is adapted from maps published by Reuters in 2015.[9]. To the best knowledge of the author, this is the most detailed publicly available information on territorial control for Nigeria at the height of the conflict. This snap shot of territorial control is coded in three categories, i.e. Boko Haram control, contested areas, and government control for four dates: 25 February, 10 March, 18 March, and 24 April. The map covers 32 local government areas in the Yobe, Borno, Adamawa states: Abadam, Askira/Uba, Bama, Bayo, Biu, Chibok, Damboa, Dikwa, Geidam, Gubio, Gujba, Gulani, Guzamala, Gwoza, Hawul, Jere, Kaga, Kala/Balge, Konduga, Kukawa, Kwaya Kusar, Madagali, Mafa, Magumeri, Maidugur, Marte, Michika,

[9]See `http://blogs.reuters.com/data-dive/2015/05/05/mapping-boko-harams-decline-in-nigeria/`, accessed 24 October 2018

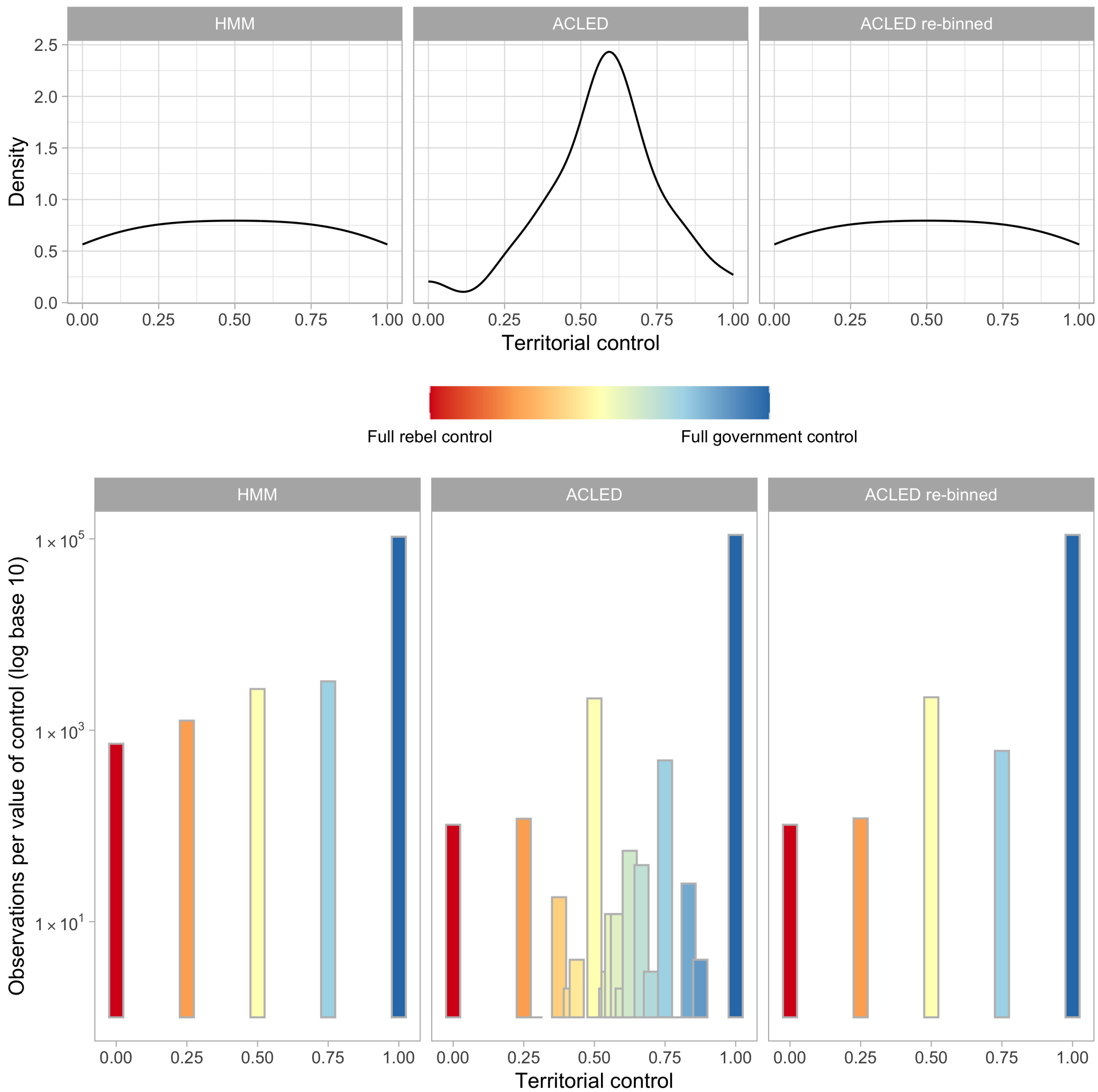


Figure 12. Density plot and histogram of HMM estimates and ACLED validation data. Values for the histogram are presented in log terms (base 10). For each panel, the number of observations sums to N = 113160 (943 grid cells × 120 months). For ACLED, the 6-month threshold is used the construct the validation set.

Mobbar, Monguno, Ngala, Nganzai, Shani. Gwoza is coded as being under rebel control on 24 April 2015 because it contains the Boko Haram stronghold in the Sambisa forest.

A number of coding choices are necessary in order to be able to compare the snap shots from Reuters with my estimates of territorial control. The first coding choice pertains to the level of spatial aggregation in the Reuters data. Reuters codes a discrete value of territorial control for each administrative area at each time point. My model yields territorial control estimates for 0.25 decimal degree minimum diameter hexagonal grid cells. I re-compute observed levels of territorial control from Reuters to match the resolution of the HMM estimates. To this end, I re-code discrete levels of territorial control in the Reuters data to match the numerical re-coding of the HMM estimates, with 0 indicating Boko Haram control, 0.5 indicating contested areas, and 1 indicating government control. The first three rows in Figure 13 illustrate the original Reuters data (top row) and two alternative gridded versions of the data. In the second row, a grid cell is coded based on the coding of the largest area of the original Reuters map contained within a given cell. For example, if 60% of the area within a grid cell were coded as contested and 40% coded as government controlled in the Reuters map, the grid cell in row two would be coded as contested. In the third row, I instead compute a cell's value as a weighted average. Using the example above, if a cell was coded as 60% contested and 40% government controlled, this cell would receive a re-computed territorial control value of $0.6 * (0.5) + 0.4 * (1) = 0.7$.

The second coding choice pertains to the recoding of HMM estimates from a 5-category variable $Q = \{R, DR, D, DG, G\}$ to a three-category variable to match the categories of the Reuters data. Again, I compute two alternative versions. In row four in Figure 13, I code areas that are estimated to be disputed but closer to rebel control ($DR$) and those that are disputed but closer to government control ($DG$) as being under the full control of the rebels ($R$) or the government ($G$), respectively. In row five, I code $DR$ and $DG$ as disputed ($D$). To compute error rates for my territorial control estimates, I again use numerical expressions of the discrete values $Q_{num} = \{0, 0.25, 0.5, 0.75, 1\}$, as outlined in Table I in the main manuscript.

A visual comparison of the plots in Figure 13 shows that the HMM estimates are available at a much more fine-grained spatial level as compared to the maps produced by Reuters. They show changes in territorial control over time, but these changes do not necessarily map onto the spatial and temporal dynamics observed in the Reuters data. In particular, while the map from Reuters suggests an almost complete loss of Boko Haram territorial control by April 2015, the monthly level HMM estimates do not reflect this sudden complete loss of control and instead code a large portion of the area as highly contested. The HMM estimates also fail to pick up the small Boko Haram stronghold that remains in the southwest of the area of observation for most grid cells and months. To numerically compare the HMM estimates with the information from Reuters, I compute the mean squared error (MSE) between the monthly grid-level data from Reuters and the HMM estimates. MSE is computed as the average difference between the HMM estimates and Reuters figures, for each alternative of re-computing the data in each time window across all grid cells, indexed by $i = 1, \ldots, N$.

$$MSE = \frac{1}{N}\sum_{i=1}^{N}(HMM_i - Reuters_i)^2$$

Figure 14 shows that the MSE differs significantly across the alternative ways of re-coding the Reuters and HMM data to make comparisons, and different time points. Recoding disputed areas that are closer to the control of one of the belligerents ($DR$ and $DG$) as highly contested ($D$) has among the lowest MSEs. The error rate is also lower for April than the other time points in the data. Overall, however, I observe a significant difference between the information from Reuters and my HMM estimates. As mentioned in the main manuscript, annual averages over monthly HMM estimates appear a lot less volatile and future research should incorporate the variation of monthly estimates as uncertainty into future models of territorial control. The accuracy of the HMM estimates may be augmented as future scholars gain access to more "ground truth" data of territorial control that can be used to inform model parameters.

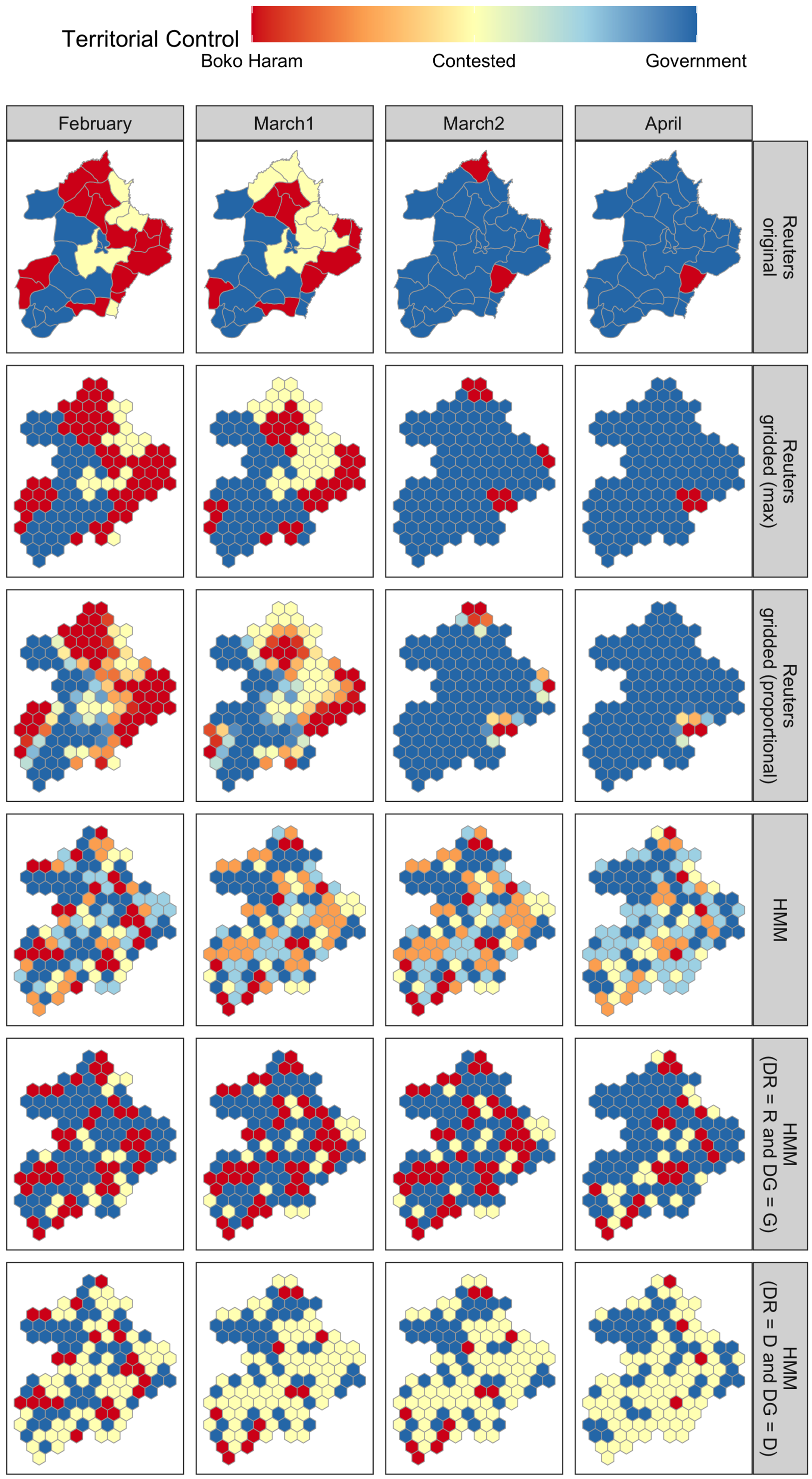


Figure 13. Comparison of HMM estimates with maps of territorial control in 32 local government areas in Nigeria in 2015 from Reuters. Please note that because the HMM is estimated at the monthly level and Reuters provides two maps for March (March 10 and March 18), I plot the March HMM estimates twice.

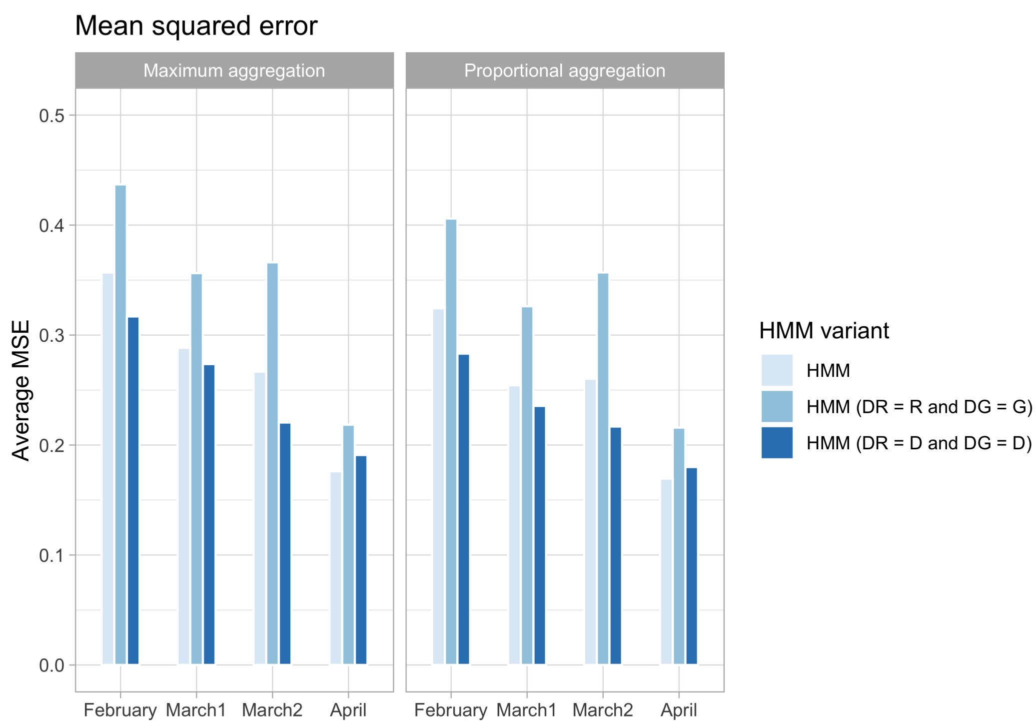


Figure 14. Mean squared errors for the comparison of the Reuters data and monthly HMM estimates in Figure 13.

# G Limitations & future research

Due to space constraints in the main paper, in the section below I discuss in more detail the limitations of the current paper and avenues for future research.

## G.1 Sensitivity of results to emission probabilities

Due to a lack of "ground truth" data that the parameters could be learned from, the emission probabilities in main text Table IV are derived heuristically. Thus, the question arises how sensitive the results are to changes in these emission probabilities.

To address this question, I create $m = 389$ sets of random emission probabilities. Originally, I create $m_o = 500$ sets of random samples of size $n = 30$ of a vector `c(1, 2, 3, 4)` with probabilities `c(0.6, 0.175, 0.175, 0.05)` and then compute the relative frequency of the vector elements to obtain random draws of the original emission probabilities that add up to one. I end up with a sample of $m = 389$, because draws in which a probability value from $\mathbf{\Phi} = \{0.6, 0.175, 0.175, 0.05\}$ is not sampled at least once are discarded to prevent any emission probabilities being set to zero. Thus, each value has a minimum emission probability of $\phi$ of $\frac{1}{30} \approx 0.033$. Increasing the number of sampled values above $n = 30$ would decrease the number of discarded draws, decrease the minimum probability of each entry to the emission matrix below 0.033, but also decrease the standard deviations of the resulting emission probabilities. At $n = 30$, the draws have the following standard deviations:

| Original probability value | Standard deviation after $m = 389$ draws |
|---|---|
| 0.600 | 0.09 |
| 0.175 | 0.07 |
| 0.175 | 0.07 |
| 0.050 | 0.03 |

I create a set of $m = 389$ emission matrices from the sets of randomly sampled probabilities. Note that because I independently sample the probability value of 0.175 twice, each draw contains two potentially non-identical random probability values for the second and third element of the vector of matrix entries.[10] This drops the assumption in the main paper that the probabilities for the second and third most likely emission, given the underlying true state of territorial control, are equal.

I then run the HMM on each of the $m = 389$ emission matrices and combine the results using Rubin's (1987) rules. The parameter of interest $\mu_i$ is the yearly mean of territorial control in each grid cell $i$. The pooled parameter estimate $\bar{\mu}$ is computed as the pooled mean, that is the average yearly mean over all $m = 389$ draws.

$$\bar{\mu} = \frac{1}{m}\left(\sum_{i=1}^{m} \mu_i\right)$$

The within variance $\sigma_W^2$ is computed as the average of the squared standard error, i.e. the annual standard deviation $\sigma_i$ divided by the square root of the number of observations per year and grid cell, for each yearly mean $\mu_i$.

$$\sigma_W^2 = \frac{1}{m}\left(\sum_{i=1}^{m}\left[\frac{\sigma_i}{\sqrt{12}}\right]^2\right)$$

The between variance $\sigma_B^2$ in computed as the sum of squared deviations of each pooled yearly average $\mu_i$ from the pooled mean $\bar{\mu}$, divided by the number of individual estimates minus one.

$$\sigma_W^2 = \frac{\sum_{i=1}^{m}(\mu_i - \bar{\mu})^2}{m-1}$$

The total standard deviation $\sigma_T$ is then computed as the square root of the total variance.

$$\sigma_T = \sqrt{\sigma_W^2 + \sigma_W^2 + \frac{\sigma_W^2}{m}}$$

Figures 16 and 17 present annual averages $\bar{\mu}$ and 95% confidence intervals (computed as 1.96 times the total standard deviation $\sigma_T$) for territorial control estimates of each grid cell in NE

[10] I randomly assign the sampled probability values for the original 0.175 probability to the second and third highest elements in each row of the emission matrices.

Nigeria 2008–2017 over all $m$ samples. The graphs show that estimates of full government control (presented in blue, numerical value closer to 1) are a lot less sensitive to the choice of emission matrix than levels of rebel control (presented in red, numerical value closer to 0), or contestation (presented in yellow, numerical value closer to 0.5). Figure 15 plots the pooled annual estimates $\mu_i$ of territorial control against the total standard deviation $\sigma_T$. It shows that levels of contestation are, on average, the most sensitive to the choice of emission parameters, followed by levels of rebel control. Future research should seek to learn the emission probabilities from data, as those might become available, to reduce the sensitivity of the results to parameter choices.

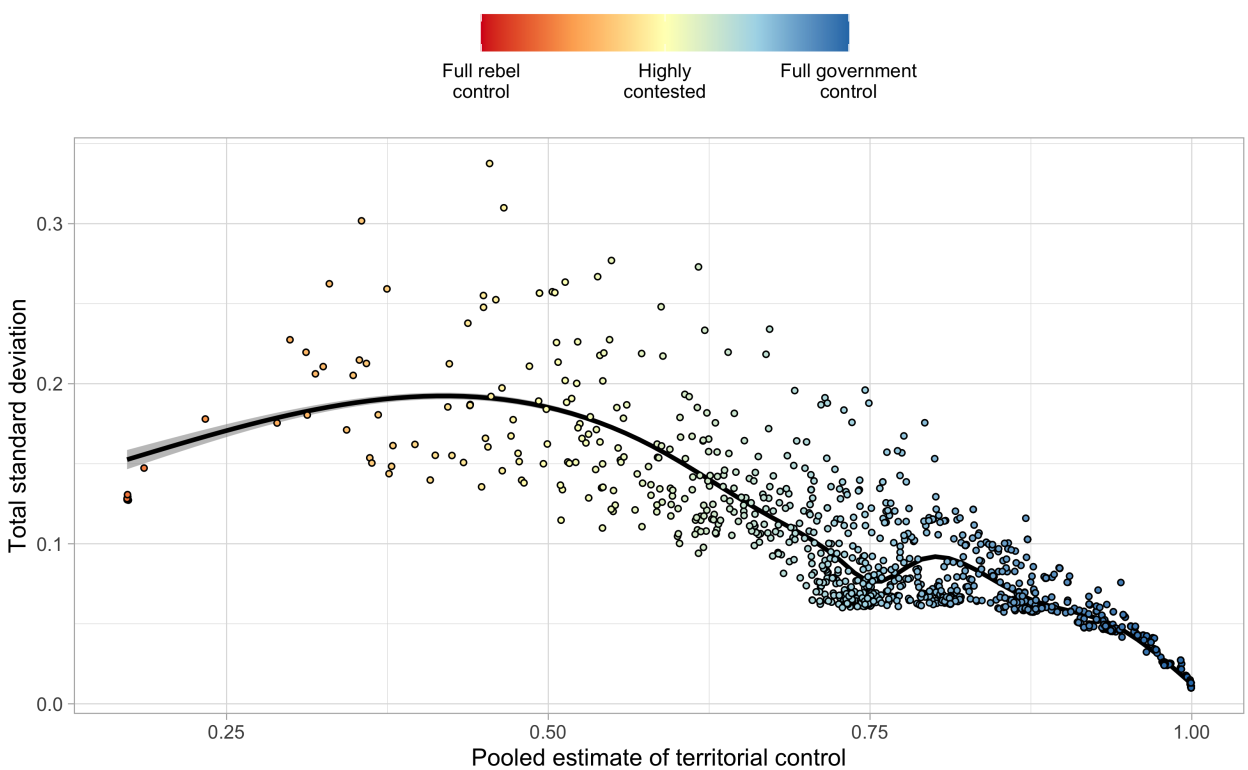


Figure 15. Relationship between the pooled estimate of annual territorial control $\mu_i$ and the total standard deviation $\sigma_T$ of the estimate across $m = 389$ randomly sampled emission matrices for NE Nigeria 2008–2017. The black line represents a generalized additive model smoothed trend. Levels of contestation are estimated with the highest uncertainty.

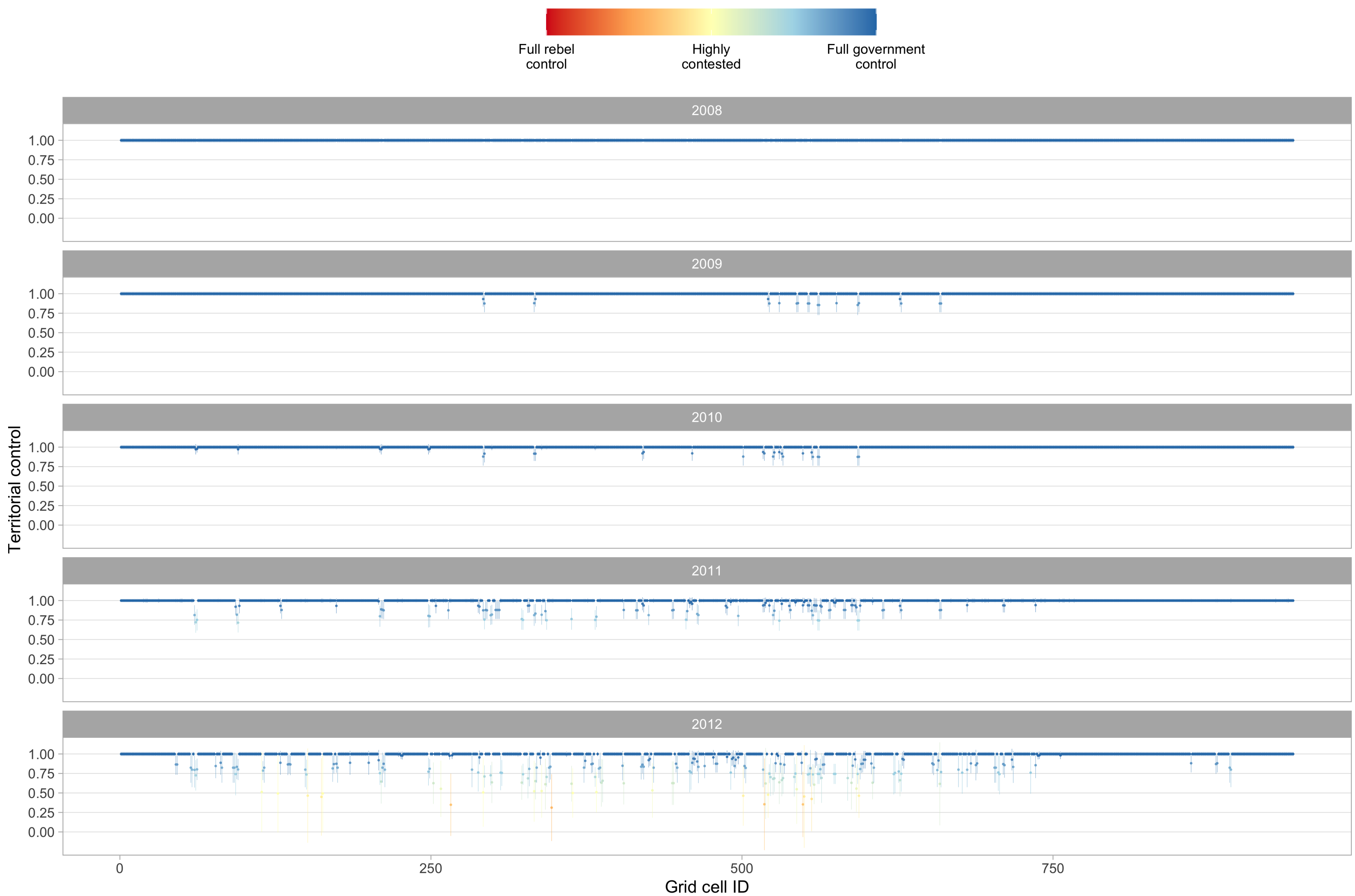


Figure 16. Sensitivity of estimates to changes in the matrix of emission probabilities. Presented are pooled annual averages of territorial control estimates per grid cell with 95% confidence intervals over $m = 389$ randomly sampled emission matrices for NE Nigeria 2008–2017. The samples are combined using Rubin's (1987) rules.

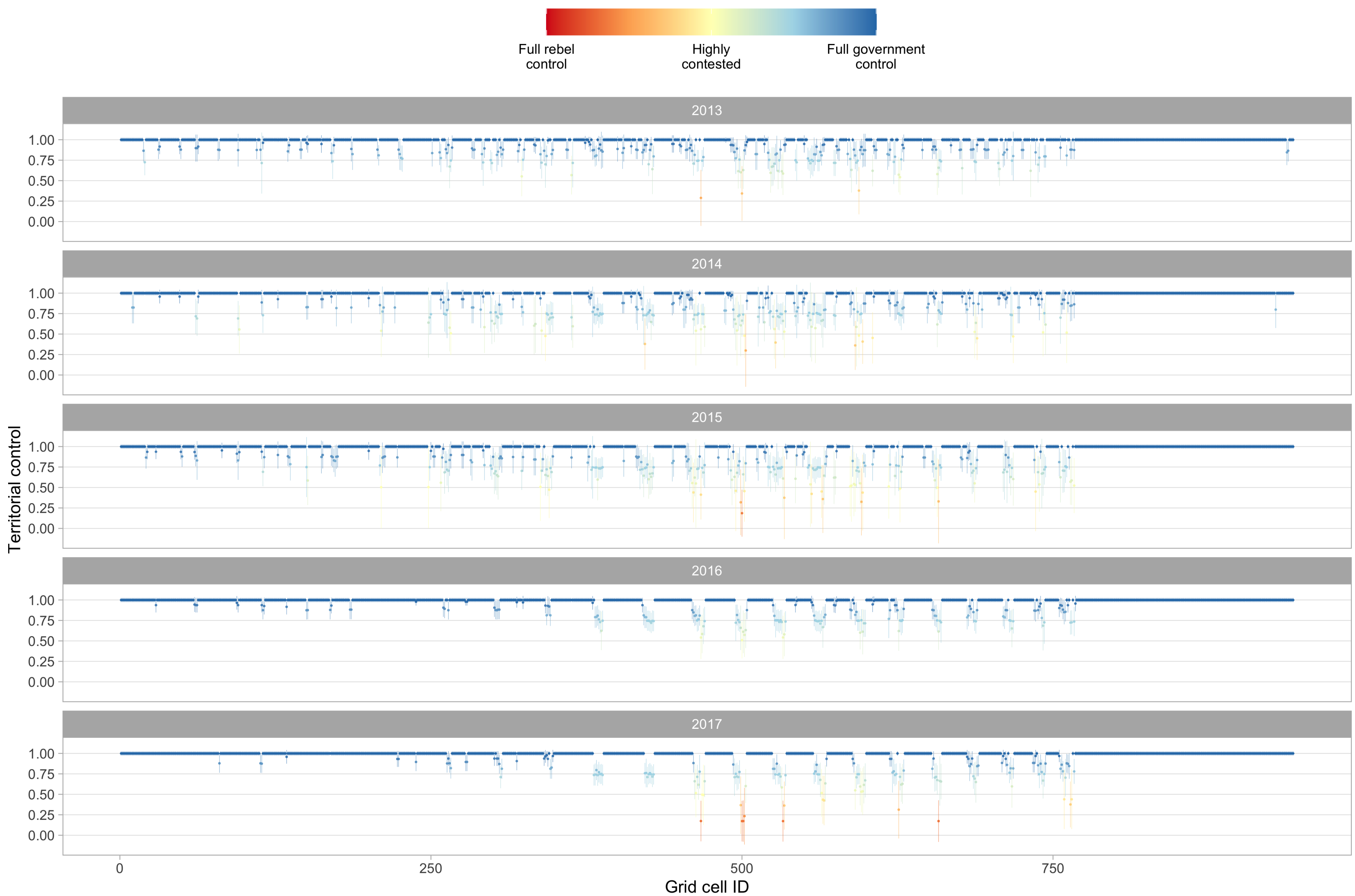


Figure 17. Sensitivity of estimates to changes in the matrix of emission probabilities. Presented are pooled annual averages of territorial control estimates per grid cell with 95% confidence intervals over $m = 389$ randomly sampled emission matrices for NE Nigeria 2008–2017. The samples are combined using Rubin's (1987) rules.

## G.2 Varying the margin parameter $m$

Below, I investigate the mechanics of the model with respect to sensitivity of the results to the margin parameter $m$. Recall the coding procedure for observed emissions in the main manuscript (Table II) in the main manuscript. The parameter $m$ controls the amount of overlap between terrorist and conventional tactics necessary to lead to the coding an observed emission of $O3$ (i.e. similar non-zero levels of exposure), and consequently also $O2$ and $O4$, see Table II in the main manuscript. A higher level of $m$ increases the number of observations that are coded as $O3$, relative to the alternative values of $O2$ or $O4$.

In figure 18, I overlay the simulated emission values with the observed draws for from a zero-inflated Poisson distribution for conventional fighting and terrorism for each grid cell-month in Colombia and Nigeria. The graph shows that the density distribution of observed draws from a zero-inflated Poisson distribution in Colombia is much narrower (i.e. values for both conventional fighting and terrorism are much closer to 1), as compared to Nigeria. For Colombia, the median value for conventional fighting is $\text{median}(C_{it}) = 0.98$ and $\text{median}(T_{it}) = 0.98$ for terrorism. For the Nigeria data, the density of observed values is farther away from 1 and more skewed (the median value for conventional fighting is $\text{median}(C_{it}) = 0.95$ and $\text{median}(T_{it}) = 0.93$ for terrorism).

Figure 18 reveals that the 'tighter' decision space for emissions to be coded as $o = O3$ (using $m = 0.025$) appears appropriate for the comparatively 'narrower' joint distribution of conventional fighting and terrorism observed in the case of Colombia (row 2, column 1). Widening the decision space would cause the bulk of Colombia emissions to be coded as $o = O3$. In contrast, in the case of Nigeria (row 2, column 2), the 'wider' joint distribution of terrorism and conventional fighting in combination with the 'tighter' decision space for emissions (using $m = 0.025$) causes significantly fewer observations to be coded as $o = O3$. Increasing the decision margin to $m = 0.05$ increases the amount of observations to be coded as $o = O3$ and appears appropriate given the underlying shape of the joint distribution of observed tactics in the case of Nigeria (row 3, column 2).

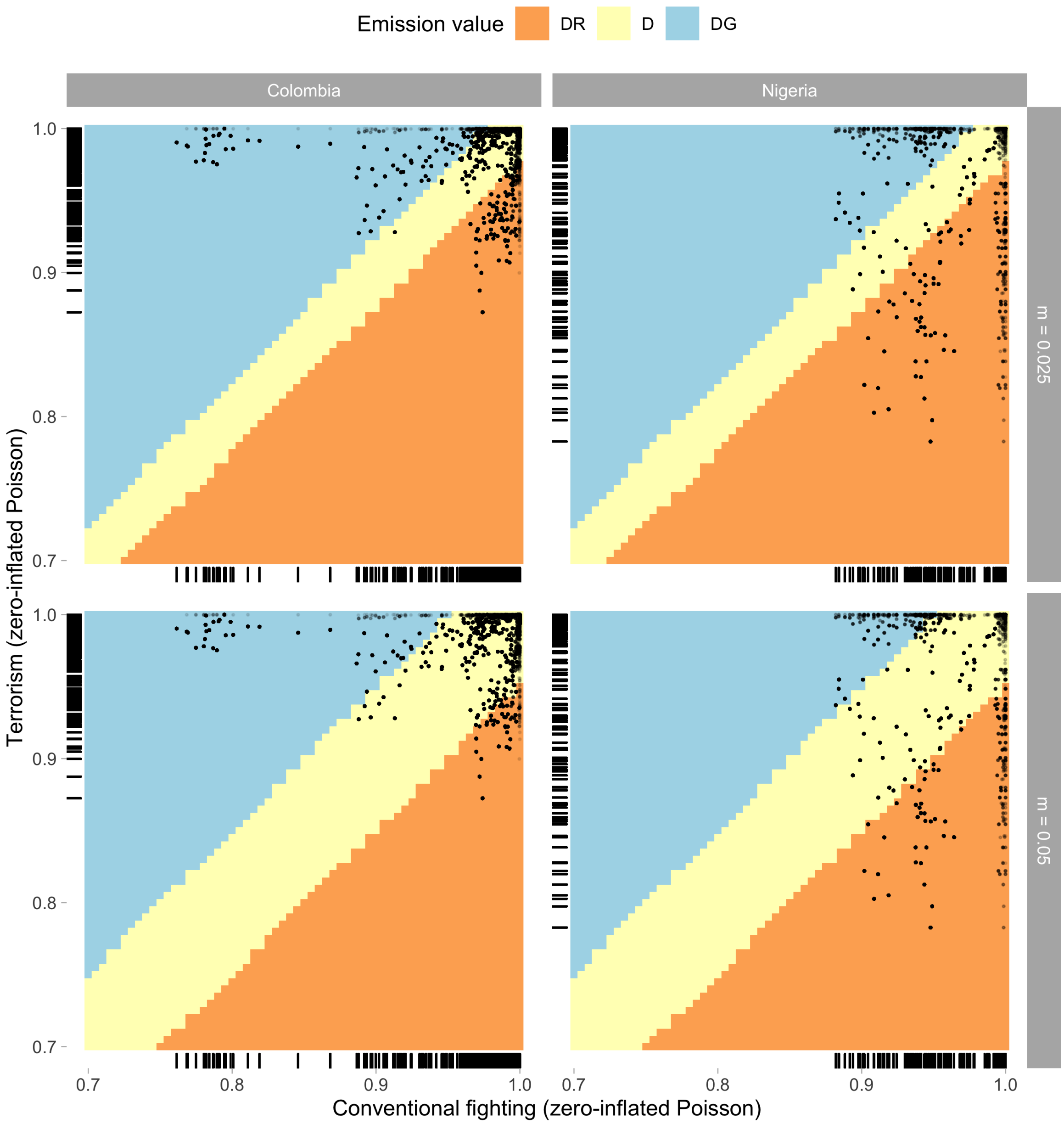


Figure 18. Simulated emission states $o = \{O2, O3, O4\}$ for all possible combinations of $C^*$ and $T^*$, overlaid with the observed distribution of $C_{it}$ and $T_{it}$ in Nigeria and Colombia and alternative margin parameters $m$.

Two innovations in future work (as stated in the article and online appendix) are likely to help reduce the sensitivity of the results to researcher-specified tuning parameters, such as the margin of overlap parameter $m$. First, future work should seek to learn these parameters using training data. In particular, the necessity to adjust the margin of overlap to the country-context (and more explicitly the underlying joint distribution of conventional and terror tactics) should be explored. Second, and in connection to using training data to learn model parameters, the utilization of alternative methods that allow for continuous inputs and continuous outputs of the model, such as Kalman filters, would further reduce the reliance of the model on researcher-specified tuning parameters in future iterations of this project.

## G.3 Potential bias due to underreporting of events

Bias in conflict event datasets due to reporting error is well documented in the existing literature (Weidmann, 2016; Eck, 2012). The identification of territorial control in the theoretical model and estimation strategy relies on variation in the co-occurrence of events that are indicative of conventional guerrilla fighting versus terrorist tactics. To assess this variation in the co-occurrence of events using different tactics, I compare probabilities from a zero-inflated Poisson distribution, with the monthly means of observed events for guerrilla fighting and terrorist tactics across the whole study region (separately for Nigeria and Colombia) as the parameter $\lambda$, i.e. the expected number of occurrences. Comparing probabilities from a zero-inflated poisson, rather than the absolute number of events, allows me to account for spatial and temporal differences in the intensity of conflict. This is important, because the theoretical model guides only how the *co-occurrence* of conventional guerrilla versus terrorist tactics relates to levels of territorial control. It is not informative as to how the overall level of violence in an area relates to different levels of territorial control.

This measurement approach also helps guard against some bias that could be caused by the underreporting of events. To the extent that both types of rebel tactics are similarly influenced by underreporting, this should not significantly bias the results.[11] The example in Figure 19 below illustrates this. The bias is set to affect terrorism and conventional guerrilla tactics similarly to reduce the observed (bias) average by 50%. Suppose in a given month we observe one event that is indicative of terrorist tactics and no event that is indicative of terrorist tactics.[12] Given the underlying true means of $E_{true}^{Terrorism} = 0.7$ and $E_{true}^{Conventional} = 0.3$ (solid lines), the emission would be coded as higher use of terrorism than conventional fighting, i.e. $O4$. The same emission $O4$ would be coded if the average of conventional and terrorist tactics are affected by underreporting at approximately the same magnitude, because the margins of the curves with biased means of $E_{biased}^{Terrorism} = 0.35$ and $E_{biased}^{Conventional} = 0.15$ no not overlap (dashed lines).

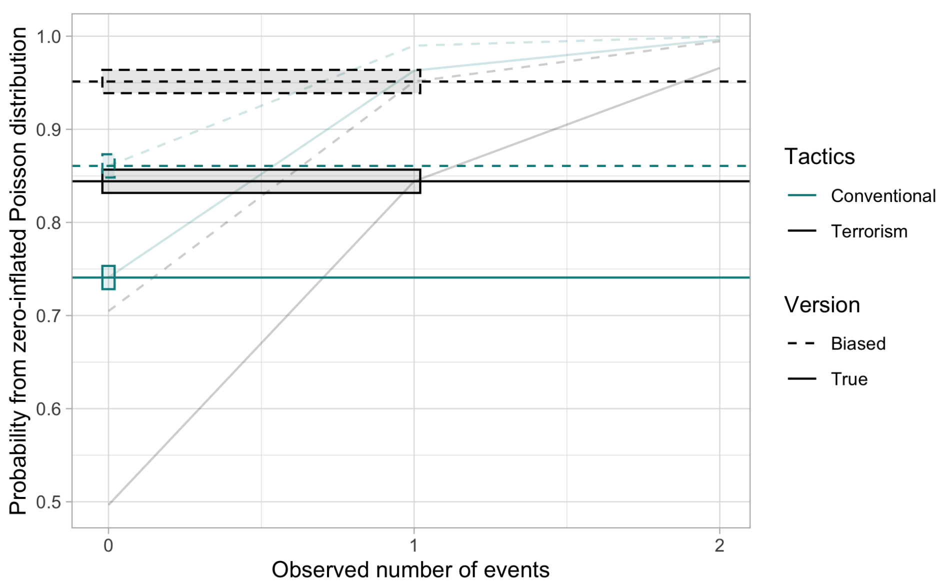


Figure 19. Illustration how underreporting might bias the results. The lines indicate probabilities from a zero-inflated Poisson distribution for 0 to 2 observed events. The shaded area indicates the approximate decision boundary around the probabilities to code an emission value of $O3$, i.e. similar levels of guerrilla and terrorist tactics. In the main manuscript, this margin is set to 0.025. The following expected number of occurrences are used in the graph above: $E_{true}^{Terrorism} = 0.7$, $E_{biased}^{Terrorism} = 0.35$, $E_{true}^{Conventional} = 0.3$, $E_{biased}^{Conventional} = 0.15$.

Given the measurement strategy above, underreporting of events is a concern for the

[11]Note that this is only true if underreporting does not cause violence to drop to zero, see below.

[12]For simplicity, in this example I assume that the cross-sectional average is biased, but the individual observations in a given grid cell are not affected by underreporting.

validity of the estimates mainly two ways. First, if no events are reported from an area that does in fact experience violence, on average, it would bias the model towards levels of complete rebel or government control, when in fact the area might be contested. This type of underreporting is particularly likely in less populated ares.[13] I drop the very sparsely populated Amazon and Orinoco natural regions from the Colombia model in order to guard against this concern to the highest degree possible.

Second, underreporting bias may influence the estimates via coding of emission probabilities if conventional and terrorist tactics are affected differently. For an example, consider again Figure 19 above. Suppose underreporting bias affected only conventional tactics (in turquoise), but not terrorist tactics (in black). This would lower the cross-sectional average of conventional fighting, causing the probability of the zero-inflated Poisson distribution of observing no conventional events to increase (turquoise, dashed). This would cause the decision boundaries of terrorist (black, solid), and conventional tactics (turquoise, dashed) to overlap, leading to an emission coding of $O3$ due to bias in the cross-sectional average of conventional events due to underreporting. The magnitude of the effect depends on the magnitude of underreporting and the extend to which it affects terrorist and conventional tactics differently.

Assessing the extent of underreporting of conflict events is extremely difficult. For conflicts like the ones in Colombia and Nigeria, a ground truth of instances of violence, against which the events reported in publicly available data sets such as the GED and GTD could be compared, does not exist.[14] The underreporting is likely related the population density of an area. The more densely populated an area, the more likely it is that a violent event will be picked up by local news or other reporting agencies. To assess the degree to which imbalanced underreporting might be an issue, I relate observed counts of events to the pop-

[13] For example, Weidmann (2016) finds that areas with cell phone coverage, which are presumably more densely populated, are more likely to have events reported, than areas that lack coverage.

[14] See Weidmann (2016) for an example in which data from the GED was compared to military records from the SIGACT data base in Afghanistan.

ulation density in a given area.[15] Specifically, I estimate the following model via Poisson regression.

$$events = \alpha + \beta_1 population + \beta_2 terrorism + \beta_3(population \times terrorism) + \epsilon,$$

where *events* denotes the count of events in a PRIO grid cell-year,[16] *population* denotes the natural log of the sum of the PRIO grid cell population,[17] and *terrorism* is a binary variable that is 1 for events that are indicative of terrorism from the GTD database and 0 for events indicative of conventional guerrilla fighting from the GED database. For Nigeria, gridded population data is only available for the year 2010. For Colombia, gridded population data is available for the years 2000 (excluded baseline category), 2005, and 2015; thus, I include time dummies in some specifications.

Recall that underreporting is a concern for the HMM estimates only if a) it reduces observed violence to zero or b) if it affects terror versus non-terror events differently. A positive coefficient on the interaction term $\beta_3$ indicates that the effect of population density on the number of reported events differs between terror- and non-terror violence. Assuming that the effect of population density on the number of observed events is a proxy for the potential size of the underreporting bias, a positive positive coefficient on the interaction term $\beta_3$ thus provides some evidence that this bias might be imbalanced between the GED and GTD databases.

Table VII reports the results of the Poisson regressions. The results indicate that imbalanced underreporting bias is a not concern in the case of Nigeria: The coefficient of the interaction term does not reach statistical significance at the minimum 5% level. For Colombia, however, there is a potential for a bias due to imbalanced underreporting between the

[15] Subnational population estimates are available via the PRIO GRID 2.0 data at a resolution of $0.5 \times 0.5$ decimal degree cells (Tollefsen et al., 2015, 2012).

[16] I compute the number of events that are indicative of conventional guerrilla fighting (GED) versus terrorism (GTD) per PRIO grid cell.

[17] Because the area of the grid cells within a single country is approximately the same, the sum of population within a cell is exactly proportional to the population density. I use the natural log of the `pop_gpw_sum` variable from PRIO GRID 2.0 to measure population.

GED and GTD datasets. The positive interaction term between population and the terrorism dummy suggests that the effect of population density of the number of reported events is stronger for events that are indicative of terror violence, compared to non-terror violence.[18] Holding population at is mean, the predicted number of GED events per PRIO grid-cell year in Colombia is 0.25, while the predicted number of GTD events is 0.05.

The direction of the effect that this imbalance in underreporting has on the HMM estimates depends on level of observed non-terror violence as well as whether the bias is constant across the entire country.[19] Future research should explore the inclusion of variables that can serve as a proxy for the magnitude of the potential imbalance of the underreporting bias between events that are indicative of terror versus non-terror violence, for example population density, into the estimation of the HMM. A comparison between the GED and GTD data with the recently released data from the Violent Presence of Armed Actors in Colombia (ViPPA) database (Osorio et al., 2019) provides additional avenues to empirically assess the extent of the imbalance in underreporting bias for the Colombia data.

[18] On average, higher population density is associated with a higher number of observed events. For both Nigeria and Colombia, on average we observe fewer terrorist events than events that are indicative of conventional guerrilla fighting, however this difference is only statistically significant at the minimum 5% level in Colombia.

[19] Consider again the example in Figure 19. Whether the more severe underreporting in the case of terrorist violence (black, dashed) causes the decision boundaries to overlap depends on the computed zero-inflated poisson probability for conventional violence, as well as on whether the bias affects just the expected number of terrorist events (not uniformly distributed across grid cells) or the particular observed number of terrorist events in a given grid cell (uniformly distributed across grid cells).

| | *Dependent variable:* | | | | | | |
|---|---|---|---|---|---|---|---|
| | Count of events per PRIO grid cell | | | | | | |
| | Nigeria | | | Colombia | | | |
| | (1) | (2) | (3) | (4) | (5) | (6) | (7) |
| Population (ln) x Terrorism | | | 0.16 | | | 0.16** | 0.16** |
| | | | (0.36) | | | (0.05) | (0.05) |
| Population (ln) | 1.02*** | 1.02*** | 0.94*** | 0.52*** | 0.52*** | 0.49*** | 0.48*** |
| | (0.18) | (0.18) | (0.27) | (0.02) | (0.02) | (0.02) | (0.02) |
| Terrorism | | 0.13 | −1.97 | | −1.17*** | −3.04*** | −3.04*** |
| | | (0.37) | (4.93) | | (0.09) | (0.65) | (0.65) |
| 2005 | | | | 0.86*** | 0.86*** | 0.86*** | |
| | | | | (0.10) | (0.10) | (0.10) | |
| 2010 | | | | −0.14 | −0.14 | −0.14 | |
| | | | | (0.12) | (0.12) | (0.12) | |
| Constant | −16.36*** | −16.43*** | −15.31*** | −7.25*** | −6.82*** | −6.41*** | −6.06*** |
| | (2.46) | (2.47) | (3.60) | (0.27) | (0.27) | (0.30) | (0.29) |
| Observations | 624 | 624 | 624 | 2,376 | 2,376 | 2,376 | 2,376 |
| Log Likelihood | −139.80 | −139.74 | −139.64 | −1,552.11 | −1,455.55 | −1,451.10 | −1,521.39 |
| Akaike Inf. Crit. | 283.61 | 285.47 | 287.29 | 3,112.22 | 2,921.11 | 2,914.19 | 3,050.78 |

*Note:* *p<0.05; **p<0.01; ***p<0.001
Poisson regression results with standard errors in parentheses.
Nigeria estimates are for 2010 only.
Base category for year dummies for the Colombia estimates is 2000.

Table VII. Assessment of imbalance of potential underreporting bias between the GED and GTD data sets.

# H Additional figures

## H.1 Case selection

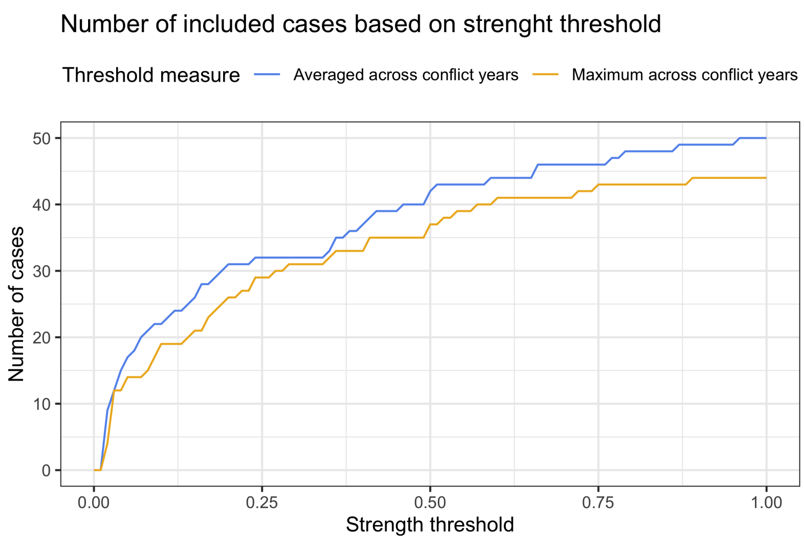


Figure 20. Number of cases that the measurement strategy can be applied to based on different thresholds of power asymmetry between the rebels and the government. Data on power asymmetry come from Polo and Gleditsch (2016).

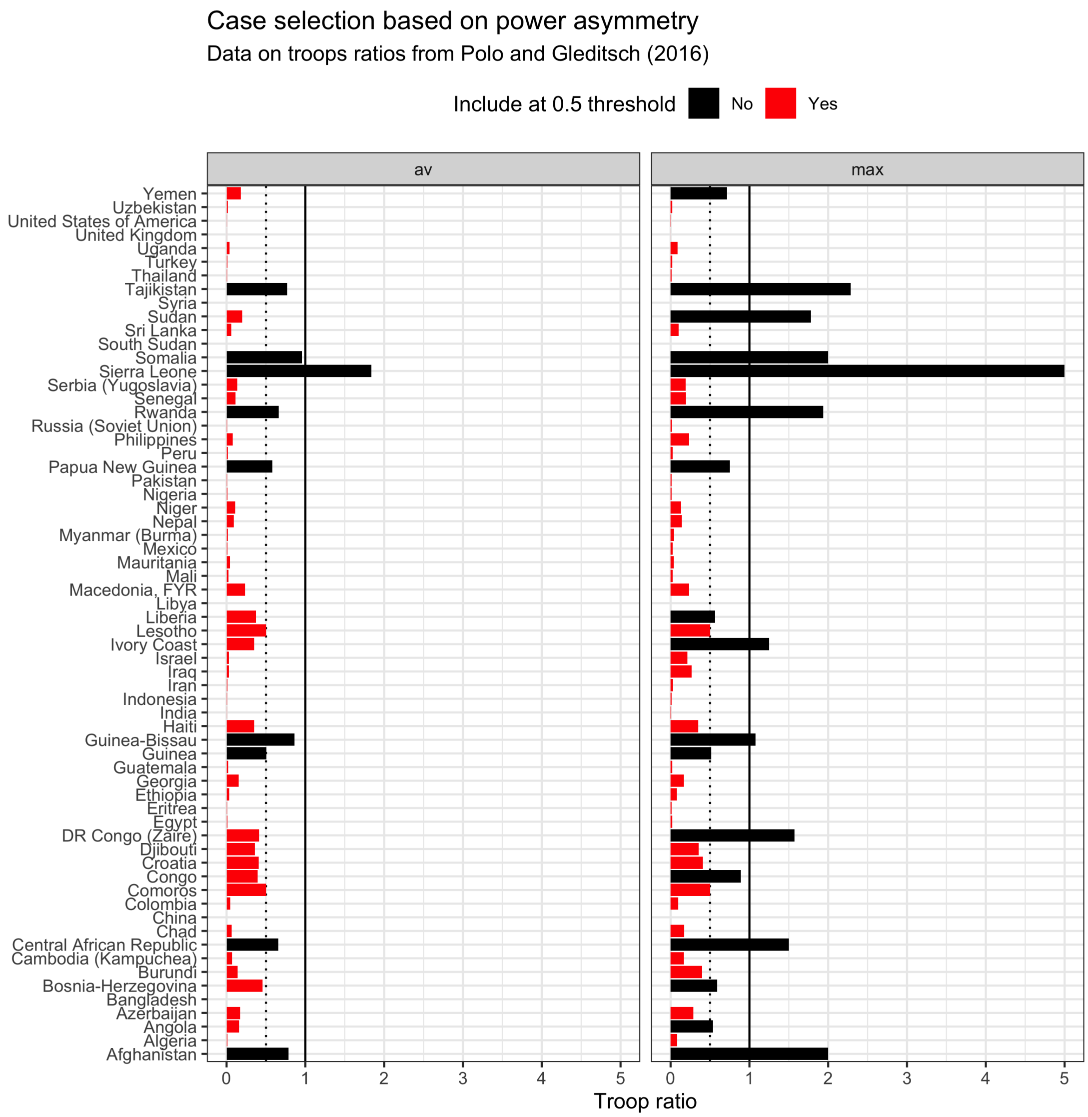


Figure 21. The graph illustrates the selection of cases for which the measurement strategy is applicable based on thresholds in average and maximum rebel-to-government troop ratios over the course of the conflict. Plotted in red are cases that would be included based on a 0.5 threshold indicating rebels that are half as strong as the government forces. Future work will investigate the determination of the most appropriate threshold.

# References


Aronson, Jacob; Deniz Ciland, Paul K Huth & James I Walsh (2017) An enhanced dataset of territorial control by conflict actors.

Asal, Victor; Luis De La Calle, Michael Findley & Joseph Young (2012) Killing civilians or holding territory? How to think about terrorism. *International Studies Review* 14(3): 475–497.

Bakker, Ryan; Jr Daniel W Hill & Will H Moore (2016) How much terror? Dissidents, governments, institutions, and the cross-national study of terror attacks. *Journal of Peace Research* 53(5): 711–726.

Croicu, Mihai & Ralph Sundberg (2017) UCDP GED codebook version 17.1.

de la Calle, Luis & Ignacio Sánchez-Cuenca (2012) Rebels without a territory: An analysis of nonterritorial conflicts in the world, 1970–1997. *Journal of Conflict Resolution* 56(4): 580–603.

Eck, Kristine (2012) In data we trust? A comparison of UCDP GED and ACLED conflict events datasets. *Cooperation and Conflict* 47(1): 124–141.

Kalyvas, Stathis N (2006) *The Logic of Violence in Civil War*. Cambridge, UK: Cambridge University Press.

National Consortium for the Study of Terrorism and Responses to Terrorism (START) (2016) Global terrorism database [data file].

Openshaw, Stanley & Peter J Taylor (1979) A millon or so correlation coefficients: Three experiments on the modifiable areal unit problem. In: Neil Wrigley (ed.) *Statistical applications in the spatial sciences*. London: Pionchapter 5, , 127–144.

Polo, Sara MT & Kristian S Gleditsch (2016) Twisting arms and sending messages: Terrorist tactics in civil war. *Journal of Peace Research* 53(6): 815–829.

Raleigh, Clionadh; Andrew Linke, Håvard Hegre & Joakim Karlsen (2010) Introducing ACLED: An armed conflict location and event dataset: Special data feature. *Journal of Peace Research* 47(5): 651–660.

Sauter, Melanie S (2017). Dangerous Territory. A subnational study on how territorial control affects violence against aid workers in Africa. Master's thesis University of Oslo.

Wimmer, Andreas & Chris Miner (2019) The strategic logic of ethnoterritorial competition: Violence against civilians in Africa's civil wars. *Journal of Global Security Studies*.